Note:
This is the author accepted version of the paper published in Quaternary Geochronology (2019; 51: 140-154, doi:10.1016/j.quageo.2019.02.007).

New developments in the radiocarbon dating of mud wasp nests

Damien Finch[1*], Andrew Gleadow[1], Janet Hergt[1], Vladimir A Levchenko[2], David Fink[2]

1 The School of Earth Sciences, McCoy Building, The University of Melbourne, Parkville, VIC Australia 3010

2 Australian Nuclear Science and Technology Organisation, Locked Bag 2001, Kirrawee, DC 2232, Australia

* Corresponding author: damien.finch@unimelb.edu.au

Declarations of interest: none

Keywords

Radiocarbon dating; rock art; mud wasp nests; charcoal; pretreatment protocols; Kimberley Western Australia; Quaternary; Geochronology;

Abstract

This paper reports on the development of radiocarbon dating of mud wasp nests to provide age estimates for rock art and other anthropogenic modifications to the surfaces of open rock shelters.

Over 150 rock shelters in the remote Kimberley region of Western Australia were visited in five field seasons. Mud wasp nest samples were collected from 108 sites. Thirty newly constructed wasp nests were collected to understand their initial composition and to determine the major sources of carbon. Charcoal-rich fractions extracted from 9 modern nests were radiocarbon dated and, whilst most were of zero age, some were found to be up to 1000 years old with the mean age being 255 years.

Of the old wasp nest samples, 120 were utilised in the experiments reported here. A variety of different physical and chemical pretreatment methods were explored but small sample sizes and low carbon concentrations limit the range of techniques that can be used in practice. The radiocarbon ages measured on the 75 nest samples that contained sufficient carbon for analysis ranged from Modern to just over 20 cal ka BP. Half of these nests were older than 8 cal ka BP and 20% were older than 11 cal ka BP. Even allowing for the inherent uncertainties due to any inbuilt carbon age, the method is capable of producing useful age estimates for rock art and other features of archaeological interest, in relatively open rock shelters.

1 Introduction

Rock shelters are often a focus of archaeological excavations as they were favoured sites for habitation and cultural practices. A range of dating techniques are available to analyse associated organic material or sediments thereby providing a chronological context for the excavated sequence. Above ground, people may have created grinding hollows, abraded grooves, cupules, petroglyphs and pictograms but such features are only rarely amenable to dating with current techniques. Therefore, it is largely impossible to place these features in a temporal context or to make a chronological link to excavated deposits, so the archaeological record of the site is inchoate. Here, we report on the development of a method that can be more widely deployed to provide useful age estimates for such features.

Mud dauber wasps are found throughout the world (Naumann 1983: 134) and their nests are common on rock surfaces. Rock shelters serve as protection for wasp nests, so nests are sometimes found on the same surfaces used by people for rock art and domestic activity. Optically-stimulated luminescence (OSL) dates on quartz grains in mud wasp nests overlying rock art have established that mineralised mud wasp nests can survive in open rock shelters for tens of thousands of years (Roberts et al. 1997, Yoshida et al. 2003). However, the application of OSL is greatly restricted because it requires old wasp nests that are still large enough to shield inner quartz grains from sunlight and such nests are rare (Aubert 2012: 576, Ross et al. 2016: 28). On the other hand, smaller stumps of old, often indurated, nests are relatively abundant.

Mud collected by wasps contains sand, clay and a variety of organic materials. The carbon composition of wasp nests will change over time as any plant matter in the mud decomposes, the outer surface weathers away, dust accumulates, and, potentially, the nest becomes mineralised. The remnant nest will also be subject to the action of bacteria, algae and fungi (Ridges et al. 2000). The critical challenge in estimating when the nest was constructed is to isolate a source of carbon for which an age can be reliably related to the construction event (Aubert 2012, Bednarik 2002, Watchman 2000). Radiocarbon dates on different organic components (e.g. wood, charcoal, pollen, plant matter) within a sediment sample have been shown to differ significantly because they originate from different sources of different age (Brock et al. 2010: 625). Early attempts to radiocarbon date a specific component from wasp nests focussed on pollen but older nests were generally found to

contain too little pollen for analysis (Roberts et al. 1997, 2000, Yoshida et al. 2003). To determine what other sources of carbon may be more suitable targets for dating we need to understand the carbon-bearing components initially present and then the broad range of diagenetic processes at work, post construction.

The aim of this research was to develop a technique that will provide robust age estimates for the timing of mud nest production and one that can be applied to a wide range of rock shelter surfaces. This paper covers the methodological aspects of radiocarbon dating of mud wasp nests; subsequent reports will demonstrate how the method has been applied to generating specific age estimates for rock art.

2 Approach

Open rock shelters in the remote Kimberley region of Western Australia contain an abundance of old mud wasp nests as well as a complex rock art repertoire and other evidence of human occupation (Morwood et al. 1994). More than 150 rock art sites in three Kimberley regions were visited in five field campaigns between 2015 and 2017 (see Green et al. (2017b) for details of the fieldwork areas and relevant geology). During two Wet season trips (February 2016 and March/April 2017), wasps were observed and recorded collecting mud, constructing nests and provisioning nests with prey. Samples from 30 freshly constructed (i.e. modern) wasp nests were collected as well as some of the mud or soil from source material gathered by the wasps. More than 300 old mud wasp nest fragments were collected from 105 rock shelters.

Modern nests were examined to understand the initial composition of nests and sources of carbon within them. Different carbon-bearing fractions were extracted, and radiocarbon dated to ascertain whether nests contain anything other than modern carbon at the time of construction.

Old nests were then studied to determine how diagenesis transforms this carbon and how new sources of carbon may be incorporated into the mineralised nest. Extensive mineralogical and geochemical analyses identified the range of minerals and elemental concentrations present in old nests. The results guided experimentation with a range of physical and chemical pretreatment processes prior to radiocarbon dating. These experiments tested the trade-off between removing all

possible sources of unwanted carbon and preserving sufficient carbon to allow reliable measurement of the age of the sample.

3 Methods

3.1 Field sampling

Sampling from archaeological sites was approved by relevant local Traditional Owners in the country of the Balanggarra and Dambimangarri People and under permits issued by the WA Department of Planning Lands and Heritage (Section 16 Permits 558 and 567).

Most mud wasp nests were removed using a 6mm chisel, sharply tapped with a small hammer and caught in a sheet of aluminium foil. In most cases, the nest would fracture along the same plane as the rock surface, minimising damage to surrounding surfaces. Samples were wrapped in aluminium foil then placed in individual plastic sample bags.

In the laboratory, all samples were photographed and weighed then wrapped in new aluminium foil for longer term storage. This storage foil had either been cleaned with acetone or baked overnight in a muffle furnace at 400^{o}C to remove any potential hydrocarbon lubricant contamination from the foil production process (Klingner et al. 2013).

3.2 Mineralogical and Elemental Analysis

Optical microscopy was used to examine the contents of the modern wasp nests. The total carbon and sulphur concentration and isotopic ratios of 5 modern and 13 old nests were determined using a Thermo Finnigan EA 1112 Series Flash Elemental Analyser at the Central Science Laboratory, University of Tasmania (Tables 1 and 5).

A broad range of analytical techniques were applied to old mud wasp nest samples. Typical nests were selected from those available at the time, where sufficient material was available after preparation of the sample for dating. X-ray diffraction (XRD) was used on 41 old wasp nests to determine the mineral composition and X-ray fluorescence (XRF) spectrometry on 14 of these nests to determine their major element composition. As XRD does not detect the amorphous content, 13 of the XRD samples were also analysed using XRF to understand the typical non-crystalline composition.

Scanning electron microscopy (SEM), and Laser Ablation Inductively-Coupled-Plasma Mass Spectrometry (LA-ICPMS) were used to understand the distribution and concentration of elements in nest samples. The experimental details of analytical equipment used can be found in Supplementary Information. The equipment and methods used for SEM and LA-ICPMS are described in Green et al. (2017a).

The internal structure of mineralised nests was investigated using prepared sample sections and micro Computed Tomography (micro-CT). Three old wasp nest samples were analysed using the GE Nanotom M micro-CT scanner at the School of Earth Sciences, University of Melbourne. Micro-CT was used to determine the extent to which mineralised wasp nests were open to intrusion from biological or geochemical processes. The output of the process is a three-dimensional model of the sample density.

3.3 Physical pretreatment

The aim of physical pretreatment was to remove any possible contamination on exterior surfaces of the sample. For the larger modern wasp nest samples, the outer surfaces were scraped away with a clean scalpel blade then a portion, generally closer to the base of the nest, was removed and lightly ground in a mortar.

A number of different cleaning processes were applied to the old, mineralised wasp nest samples, depending on their size. Large, solid samples had their outer surfaces removed with a clean diamond coated disk in a rotary drill. Medium sized and more fragile pieces had any obvious detritus scraped off with a sterile scalpel blade. Some small and very irregularly shaped samples were cleaned in ultrapure water using an ultrasonic bath. One third of samples were made up of small or very friable pieces with the structure of sand and were given no physical pretreatment. Where possible, the outer surfaces of under art samples (i.e. those nests underlying pigment) were more aggressively removed to further minimise the possibility of modern carbon contamination. All samples were ground in a clean mortar and placed into a 15ml or 50 ml centrifuge tube, depending on sample size.

3.4 Chemical pretreatment

3.4.1 General pretreatment protocol

Chemical pretreatment was applied to the ground samples to remove unwanted carbon compounds. Apart from the variations noted in following sections, pretreatment followed the long-established acid-base-acid (ABA) charcoal pretreatment protocol (Devries and Barendsen 1954, Hatté et al. 2001 and Supplementary Information). If the sample remaining after pretreatment was less than about 1 mg it was pipetted directly into a short silica combustion tube, then dried. Larger dried samples, up to 100 mg, were loaded into standard silica combustion tubes.

3.4.2 Modern mud wasp nests

A variety of fractions were prepared from modern wasp nests, lightly ground in a mortar. Heavy liquid separation (HLS) using either lithium heteropolytungstate (LST) or sodium polytungstate (SPT) was used on most samples at a density of 2.0 g/cm^3 to separate light and heavy fractions. Light fractions were dissected under a microscope to extract charcoal rich fractions from 11 samples. A plant material fraction for D208 was extracted in the same manner. All fractions then underwent a modified version of the pretreatment protocol outlined in 3.4.1. Initially HLS was carried out prior to ABA but in subsequent experiments the order was changed as indicated in the Pretreatment column in Table 2. Other fractions extracted from modern nest samples include some where only the first acid step was completed using 2M HCl (identified as “Acid Only” fractions). Two humic fractions (“BaseSol”) were also prepared using the supernatant from the first ABA Base step, resulting from dissolution of the sample in 0.5% NaOH, then precipitation following the addition of 2M HCl. Two samples were pretreated without undergoing HLS and one of these, D215, was split into two aliquots; one received “Acid Only” pretreatment and the other full ABA with a separate “BaseSol" fraction extracted after the first alkali treatment.

3.4.3 Old mud wasp nests

In initial experiments, old wasp nest samples received the same general chemical pretreatment process described in 3.4.1. For samples processed after the first set of results were acquired, long combustion tubes were used to load a larger mass of pretreated material, up to 300 mg, when suitably large samples were available.

Initial experiments (Sample numbers OZT445 to OZT800) on larger old wasp nest samples used HLS after the final acid step at a density of up to 2.5 g/cm^3 (LST). Samples were centrifuged at 3000 rpm for 20 minutes. Any floating material was pipetted into a separate centrifuge tube then the process was repeated. Extended centrifuge times of up to 60 minutes and speeds of up to 4000 rpm were used if the light fraction appeared to contain too little material after the initial attempts. In later experiments (samples OZU776 to OZW425), HLS was carried out after the first acid treatment using 0.5M HCl. For the final experiments, HLS was carried out after completion of the alkali step and the final acid treatment was changed to 8M or 16M HCl for a duration of at least 30 minutes at room temperature.

To experiment with alternative pretreatment protocols, a selection of some very large samples was treated with concentrated (48%) hydrofluoric acid (HF) mixed with the first HCl acid treatment in ABA processing. After the residue was rinsed, a small portion was pipetted on to a glass slide for inspection under an optical microscope.

To assess levels of potential contamination that may be introduced at any stage from pretreatment through to AMS measurement two types of reference samples were prepared. Simulated modern pseudo-nest material was created using quartz sand (Sigma-Aldrich, acid purified, 40-100 mesh, 84878) mixed with ~0.05% (by weight) ground modern charcoal (OZV994, 103.45 pMC). Simulated ancient nest material was prepared by mixing quartz sand and ~0.3% charcoal prepared from ~8 million-year-old fossil wood (OZO022) from a coal deposit. These two materials are referred to herein as “Modern pseudo-nest” and “Ancient pseudo-nest” samples respectively.

3.4.4 Graphitisation and AMS measurement

The standard process and equipment used to convert most pretreated samples into graphite targets for accelerator mass spectrometry (AMS) measurement is described by Hua et al (2001, 2004) and in the Supplementary Information. Some 33 samples used the Australian Nuclear Science and Technology Organisation’s (ANSTO) microconventional furnace (MCF) facility for ultra-small samples (Yang and Smith 2016, Yang et al. 2013). The carbon isotope ratios were measured using ANSTO’s Accelerator Mass Spectrometers (AMS) (Fink et al. 2004, Wilcken et al. 2015).

4 Results

4.1 Modern mud wasp nests

While weathering and diagenesis transform nest morphology, careful study of the different types of modern nests aids the identification of suitable ancient wasp nests in the field. Original nests can be re-used by other species of wasps and bees so different parts of a remnant nest may have been constructed at different times. Observations of a wide variety of younger nests aids the identification (and avoidance) of such problematic samples.

Out of the 8 fieldwork sessions, wasps were observed collecting mud or building nests only in the two Wet season visits, consistent with Naumann's observation that nesting gradually ceases during the Dry season (1983 :135). Wasps were observed collecting mud from 5 sites; all within rock shelters. Two sites were on the sides of small ephemeral pools of water. Of the other 3 sites, one was a muddy slope in a very dark cavity deep within the rock shelter. As others have also observed (Bednarik 2014: 227), the quartz grains in mud collected without exposure to sunlight may not be "reset" for the purposes of OSL dating so their OSL age would not be the same as the age of the nest. The other two sites were flat areas where sandy soil had accumulated. The soil here was dry and yet the mud ball formed by the wasp (typically 2 -3 mm diameter) was wet. These wasps did not appear to carry water externally to the mud collection site and the volume of water required is significant compared to the size of the wasp (see Supplementary Information video). This suggests the wasp initially ingested water elsewhere before regurgitating it at the point of soil collection, supporting reports of wasps sometimes mixing saliva with the material collected (Naumann 1983: 156, Polidori et al. 2005 :156 and references therein) and the detection of organic ketones in nests (Bednarik 2014 :226).

Sample	C%	Corrected $\delta^{13}C_{PDB}$
D202	2.58	-23.30
D206	0.76	-9.76
D208	0.39	-22.21
D210	1.47	-16.68
D219	0.85	-21.16
Mean	1.21	-18.62

Table 1 Analysis of carbon in modern wasp nests

Modern, single generation nests from 13 different sites were analysed to identify the main sources of carbon, particularly those likely to persist for millennia, to inform development of optimal pretreatment methods for old nests. Elemental analysis of 5 modern nests measured an average carbon concentration of just 1.2% (Table 1) and optical microscopy confirmed the major component is quartz sand. HLS was used to remove the quartz and subsequent dissection of light fractions (using a needle under binocular microscope) established that plant material and charcoal were the largest sources of carbon-bearing compounds, by volume (Figure 1). Insect sclerites were commonly found but in small volume. Very little pollen was observed in any of the light fractions.

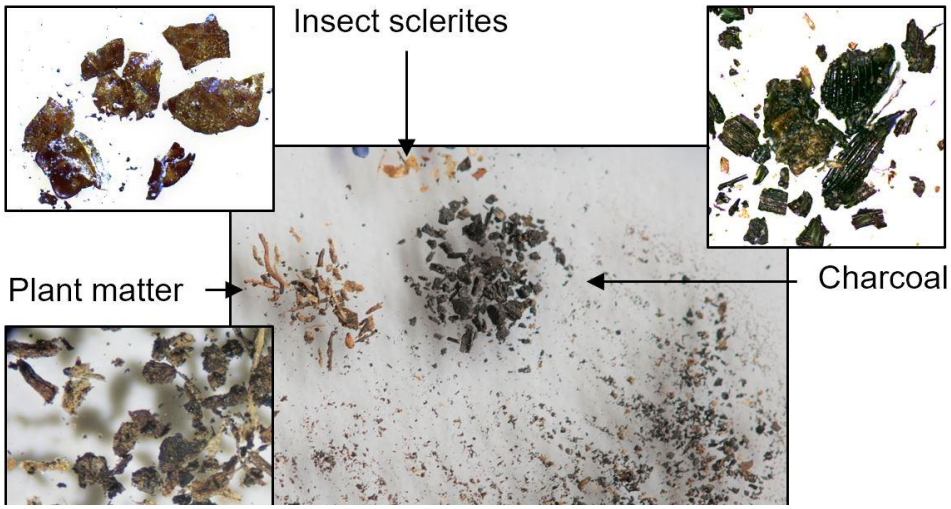

Figure 1 Light fraction of a typical modern wasp nest sorted into charcoal, plant and insect components.

Samples from 19 modern wasp nests and from 2 mud collection sites were radiocarbon dated (Table 2). All calibrated radiocarbon ages quoted herein used OxCal version 4.3.2 Bronk Ramsey (2009a, 2017) and the SHCal13 atmospheric curve (Hogg et al. 2013).

Sample Code	Laboratory Code	Sample material	Pretreatment	Fraction	Radiocarbon Age (BP)	Error (1σ)	Date calBP Median (95.4%)
D202	OZU719	Nest (S. laetum?)	HLS - ABA	Charcoal	1,090	50	950
D202	OZU720	Nest (S. laetum?)	HLS - ABA	Light	Modern		-
D204	OZU721	Nest (S. laetum?)	HLS - ABA	Charcoal	Modern		-
D204	OZU722	Nest (S. laetum?)	HLS - ABA	Light	Modern		-
D206	OZU723U1	Nest	HLS - ABA	Light	Modern		-
D206	OZU723U2	Nest	HLS - ABA	Heavy	550	35	530
D207	OZU724	Nest	ABA	All	330	60	380
D208	OZU265	Nest (S. laetum?)	HLS - ABA	Charcoal	735	30	650
D208	OZU266	Nest (S. laetum?)	HLS - A only	Heavy	1,090	30	950
D208	OZU267	Nest (S. laetum?)	HLS - A only	Light	815	25	700
D208	OZU268	Nest (S. laetum?)	HLS - ABA	Plant	Modern		-
D208	OZU730U1	Nest (S. laetum?)	ABA - HLS	Light	580	35	540
D208	OZU730U2	Nest (S. laetum?)	ABA - HLS	Heavy	680	40	600
D208	OZU730U3	Nest (S. laetum?)	A	BaseSol	935	20	790
D209	OZU725	Mud balls near D208	ABA	All	Modern		-
D210	OZU269	Nest (S. laetum?)	HLS - A only	Light	Modern		-
D211	OZU726U1	Nest (S. laetum?)	ABA - HLS	Light	315	25	370
D211	OZU726U2	Nest (S. laetum?)	ABA - HLS	Heavy	Modern		-
D212	OZU727U1	Nest	ABA - HLS	Light	Modern		-
D212	OZU727U2	Nest	ABA - HLS	Heavy	2,040	80	1,960
D213	OZU270	Nest (S. laetum?)	HLS - A only	Light	Modern		-
D215	OZU271U*	Nest (S. formosum?)	A only	All	200	30	190
D215	OZU271U1	Nest (S. formosum?)	ABA	All	115	25	70
D215	OZU271U2	Nest (S. formosum?)	A	BaseSol	100	50	90
D216	OZU728U1	Nest (S. laetum?)	ABA - HLS	Light	Modern		-
D216	OZU728U2	Nest (S. laetum?)	ABA - HLS	Heavy	Modern		-
D217	OZU729U1	Nest, resin coated	ABA - HLS	Light	Modern		-
D217	OZU729U2	Nest, resin coated	ABA - HLS	Heavy	Modern		-
D219	OZU272	Nest, resin coated	HLS - A only	Light	Modern		-
D500	OZW346	Nest, eumeninae	A - HLS - BA	Charcoal	825	20	700
D508	OZW344	Nest (S. laetum?)	A - HLS - BA	Charcoal	Modern		-
D514	OZW347	Nest (S. laetum?)	A - HLS - BA	Charcoal	Modern		-
D632	OZW349	Nest (S. laetum?)	A - HLS - BA	Charcoal	Modern		-
D670	OZW350	Nest (S. laetum?)	A - HLS - BA	Charcoal	Modern		-
D699	OZW345	Nest (S. laetum?)	A - HLS - BA	Charcoal	Modern		-
D516	OZW348	Soil from mud collection site	A - HLS - BA	Charcoal	2,110	25	2,040
D700	OZW351	Dry soil below D699	A - HLS - BA	Charcoal	Modern		-

Table 2 Radiocarbon ages and calibrated median dates for modern wasp nests and 2 associated mud sources.

The pretreatment code lists the steps taken in chemical pretreatment in the sequence indicated from left to right.

See Supplementary Information for δ13C, pMC and calibrated radiocarbon age ranges.

Of the 19 individual modern wasp nests dated, 8 contained carbon that was not modern. One of these dates, 2150 - 1750 cal BP (95% probability, 1960 cal BP median) for OZU727U2, was measured using a carbon mass of just 17µg and is considered less reliable, but the other results clearly show an inherited component contributing to a significant inbuilt average radiocarbon age for some newly constructed nests. Where heavy and light fractions from the same nest were dated, it is the heavy fraction that often contains any older carbon. In the light fractions, young plant material was a major component of all 12 and in only 3 samples does older carbon (probably from charcoal) give rise to non-modern average ages of 370, 540 and 700 cal BP (median). The ages measured for 9 charcoal fractions ranged from 0 to 950 cal BP (median probability) with a mean of 255 cal years.

Of the charcoal fractions extracted from two soil samples one was modern and the other was 2,040 years cal BP (median probability).

Age determinations on four fractions derived from sample D208 indicate that all but the plant fraction contained old carbon with the heavy fraction dated to almost 1000 cal BP. The light and charcoal-rich fractions were a few hundred years younger (Table 2). While the hand-picked, charcoal-rich fraction is dominated by macroscopic charcoal, smaller charcoal fragments were concentrated in the remaining light fraction, with some mineral coated or impregnated charcoal pieces (Bird et al. 2008: 2703) in the heavy fraction. A different portion (OZU730) of the same D208 nest was pretreated using the full ABA process. The ages for the heavy and light fractions were 540 and 600 cal BP respectively, younger than those of the previously measured portion (OZU266 and OZU267). The precipitated alkali soluble fraction (OZU730U3) for the same sample was dated to 790 cal BP (median) so the removal of this material (humic acid) during ABA processing explains the younger ages for the light and heavy fractions. Given the ages of the other fractions, the source of this humic acid is probably endogenous, diagenetically altered, charcoal rather than exogenous organic material (Ascough et al. 2011: 76).

4.2 Old mud wasp nests

4.2.1 Nest Construction

Observation of mud wasp nests at more than 150 rock shelters suggests that new nests are quickly transformed due to decomposition and weathering. There are relatively few examples of nests with intact outer surfaces (e.g. Figure 2a, e, f). The thin outer “fins” of S laetum nests (Figure 2f) and the thin outer cell walls of S formosum nests (Figure 2a) weather away rapidly and the initial structure of

the nest is lost. The common remnant nest is a distinctive oval shaped stump (e.g. Figure 2c, d, h, i) being the thicker, often mineralised mud at the base of the nest. Where mineral accretions have developed on the rock surface (Green et al., 2017b), they can thoroughly indurate and cover old nest stumps (Figure 2 i).

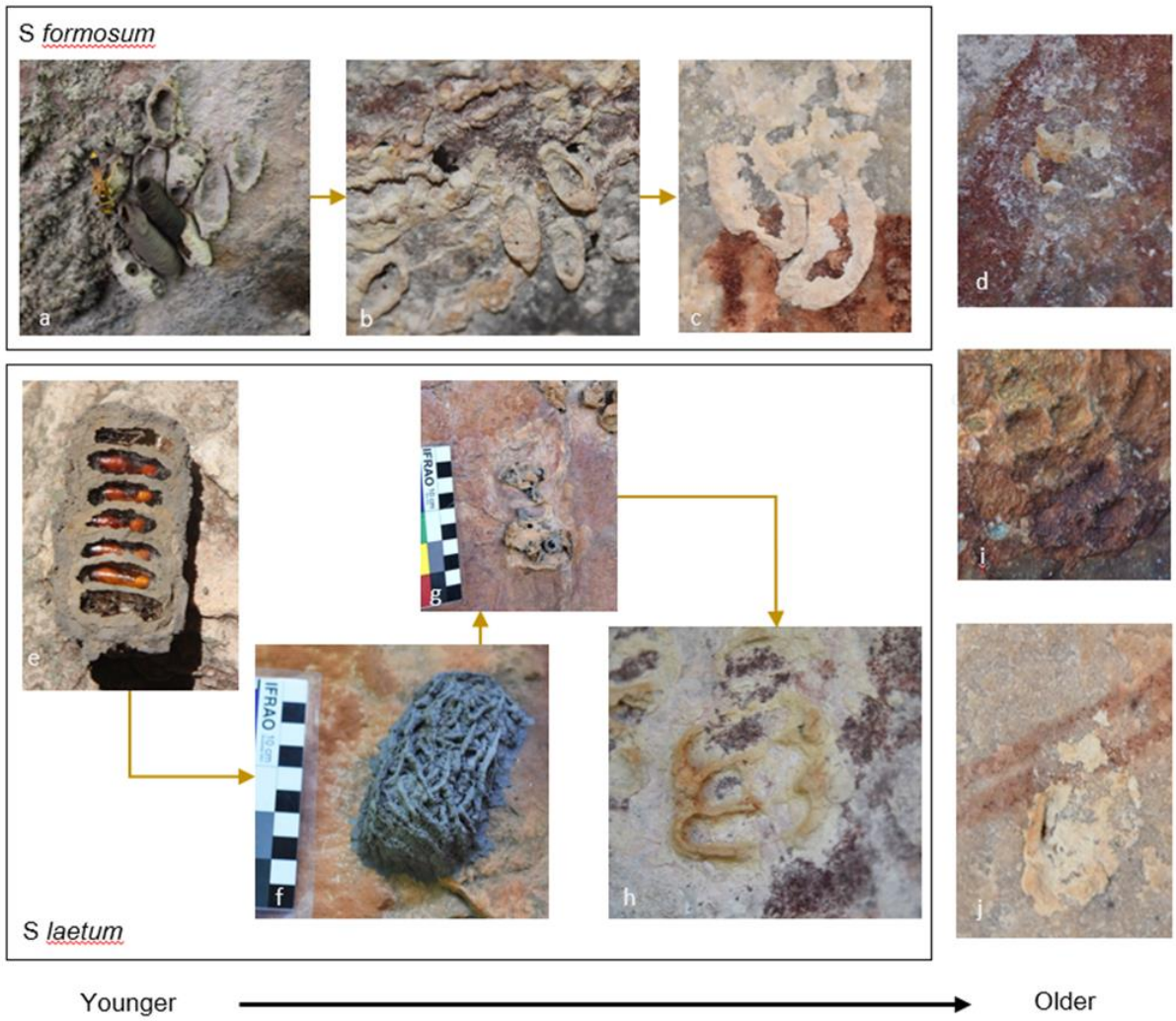

Figure 2 Nest diagenesis for two of the most common wasp species: S formosum (a - c), S laetum (e - h). (e) is the underside of a new laetum nest showing the characteristic oval shape of cells, two of which are provisioned with spiders and the other 5 having developed to the prepupal stage.

Wasps prefer to build nests in the most protected areas in Kimberley rock shelters, avoiding sunlight and wet areas, as has been reported in the Kakadu region (Naumann 1983: 135). Successive generations of wasps exhibit the same preference so new nests are often constructed on top of old ones in the most favoured locations, thereby creating thick accumulations of multi-generational nests

(Figure 3). However, in the great majority of cases, such areas are not selected for rock paintings. A typical painted panel will be more exposed and while nest stumps are still found on these surfaces they are usually dispersed and not constructed on top of older nests. Of the 30 modern wasp nests collected only one (Figure 2a) appeared to be built on the stumps of old nests. This observation is contrary to reports from other research, where it is stated that wasps prefer to build nests on top of the stumps of old nests (Bednarik 2014: 227, Roberts et al. 1997: 698, Ross et al. 2016: 7). This disagreement may be due to views about the minimum acceptable size for a nest sample. For OSL dating, substantially larger samples are required to ensure that the quartz grains have not been exposed to light, post-construction (Roberts et al. 2000: 42). These larger samples are usually only found as multi-generational nests in the more sheltered, highly favoured locations where nest density is very high (Figure 3). While large samples are also advantageous for radiocarbon dating, large intact nests are rare compared to the much more common, smaller, nest stumps found on the more exposed painted panels.

Figure 3 High density wasp nest areas. In (c), the location selected for the most recent nest (bottom) is relatively clear of other recently constructed nests and larger nest stumps.

Intact and abandoned nests may be re-used by many species of wasps and bees that do not construct complete, new nests (Naumann 1983: 175). Secondary nest builders often re-work or add mud to reshape the original cells so the ages of material at either end of the nest may be different.

Ideally, a sample for dating will be of a single generation nest, not a multi-generation or reworked nest.

4.2.2 Nest Composition

4.2.2.1 Internal structure

The internal structure of old nests was investigated to understand the potential for new carbon-bearing material to be incorporated into the nest structure.

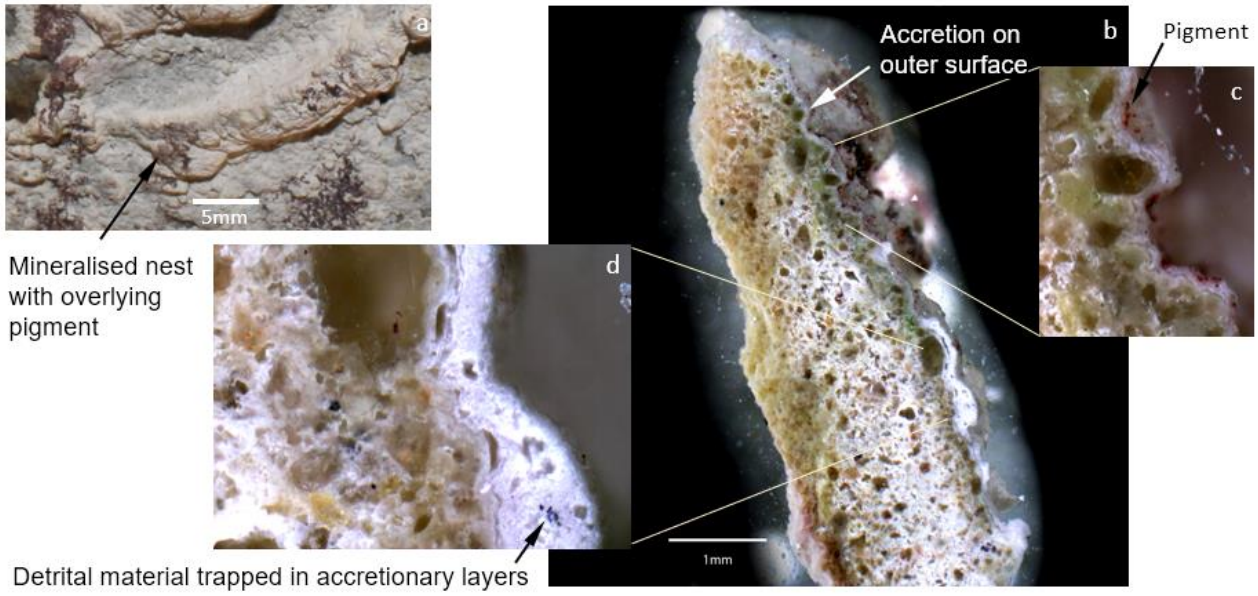

Figure 4 Mineralised wasp nest stump (a) in section (b), with overlying pigment (c), showing detrital material trapped in the accretionary layers(d)

Optical inspection of polished sections confirmed that heavily indurated nests are coated with accretionary layers (Figure 4) and that these layers can trap detrital material (Figure 4d), including charcoal. Significant amounts of charcoal embedded in mineral accretions have also been reported from other sites in the Kimberley region (Ford et al. 1994: 61). LA-ICPMS scans of nest sections show high concentrations of accretionary materials on outer surfaces and, sometimes, on the underside where mineral coatings on the rock surface have bonded with the nest (Figure 5). For larger sample pieces these coatings were removed mechanically before chemical pretreatment. This is not possible for smaller, and friable samples where chemical pretreatment will remove some sources of exogenous carbon, but not necessarily all of them.

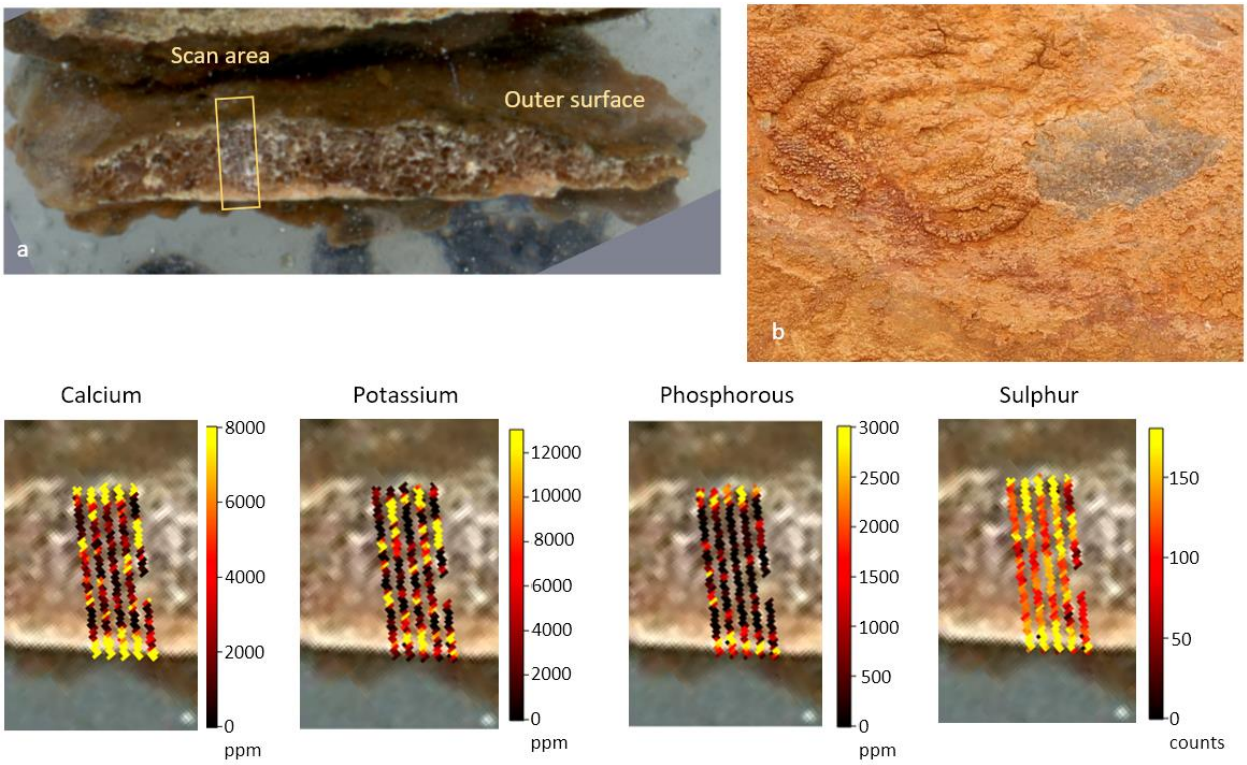

Figure 5 Distribution of Ca, K, P and S in a mineralised nest (D018). Note the warm tones through to yellow indicate increasing concentration in each case. Ca, K and P quantified using calibration against NIST SRM 612 with an estimated precision of elemental concentrations of <5%. S is illustrated on the basis of signal intensity and provides only a qualitative indication of S content.

Examination of polished sections of a range of old nests and micro-CT scans (see Supplementary Information for an example) show nest interiors to be thoroughly mineralised with few contiguous pore spaces. SEM imaging (e.g. Figure 6) shows some voids partly filled with crystalline growths. Across the range of samples imaged, mineralisation had closed off most of the pore space leaving little opportunity for later intrusion of biogenic, aeolian or fluvial contamination. This decrease in porosity is similar to that observed in buried charcoal (Bird et al. 2008: 2705).

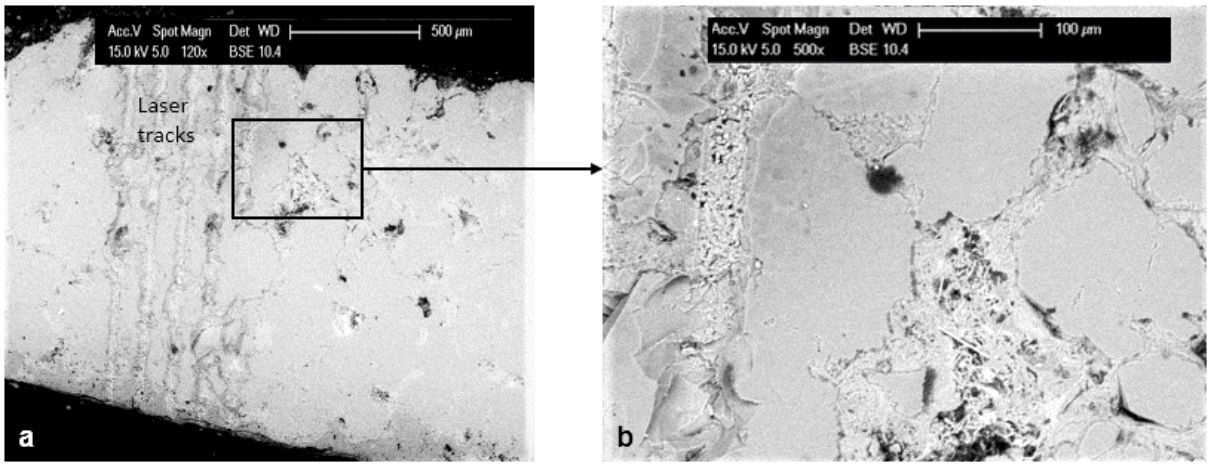

Figure 6 SEM imaging of D018, in the area around the LAICPMS scan in Figure 5. Crystalline growths evident in interstitial space in expanded view on the right

4.2.2.2 XRD

Old nests are dominantly composed of quartz, with subordinate clays from the original mud, together with traces of a range of minerals that are also found in accretions throughout Kimberley rock shelters (Green et al. 2017a, Green et al. 2017b). Of the 39 nests analysed using XRD, only 9 contained major levels (>15% by weight of crystalline content) of phases other than quartz (Supplementary Information **Error! Reference source not found.**2). These included the accretionary sulphate minerals; gypsum, alunite and polyhalite, the phosphates; taranakite and tinsleyite and the oxalate; whewellite. The highest levels of oxalates were observed in heavily indurated nests, similar to Figure 2i. The highest levels of phosphates and sulphates are associated with indurated nests from areas with thick surface mineral accretions (e.g. Figure 3a and b). Only two nests contained calcite, and only at trace levels. Apart from the insoluble oxalates (whewellite, glushinskite), calcite was the only carbon-bearing mineral detected. It is likely that calcite and the oxalate minerals are present in many samples but at levels below that detectable using XRD (<2 or 3%). One objective of the chemical pretreatment was to ensure that even trace levels of these carbon-bearing minerals were removed prior to radiocarbon dating.

4.2.2.3 XRF

As XRD does not detect amorphous minerals, the elemental composition of 14 large nest samples were analysed using XRF (Table 3).

Sample	Na_2O	MgO	Al_2O_3	SiO_2	P_2O_5	K_2O	CaO	TiO_2	Fe_2O_3
D013	0.0	0.2	4.2	85.7	0.4	0.4	0.1	0.4	1.7
D018	3.7	1.5	2.7	57.7	0.5	0.6	12.8	0.1	0.7
D025	0.4	0.3	4.8	76.2	1.4	0.3	0.3	0.3	1.5
D027	0.1	0.1	5.2	86.8	1.3	0.3	0.1	0.4	1.4
D034	4.7	1.2	5.1	63.2	9.7	1.5	3.6	0.4	2.0
D105	2.0	0.6	6.9	78.9	3.2	2.7	0.7	0.4	2.5
D131	2.4	0.4	4.7	77.7	3.8	2.5	0.6	0.5	1.4
D134	4.4	1.3	7.6	67.9	6.7	3.8	3.4	0.5	2.1
D136	0.7	0.3	6.2	81.4	1.2	1.7	0.3	0.5	1.7
D140	0.0	0.1	4.7	81.8	0.1	0.6	0.0	0.6	1.6
D147	1.1	0.5	4.0	83.8	1.2	1.7	0.3	0.3	1.4
D154	4.3	1.8	4.0	69.6	4.9	4.1	2.6	0.2	1.5
D155	1.2	0.6	8.7	75.6	0.8	2.3	0.6	0.5	2.7
PC15-01	0.9	0.3	4.0	82.0	0.3	1.7	0.3	0.4	1.4
Mean:	1.8%	0.7%	5.2%	76.3%	2.5%	1.7%	1.8%	0.4%	1.7%

Table 3 Major elements, in weight % oxides, from XRF analysis. The average MnO% was 0.03% with a maximum of 0.08% in D134. Low total compositions are due to unreported sulphur (particularly D018) and carbon (D025).

The XRF elemental analyses are broadly consistent with the XRD mineralogical analyses with no suggestion that other amorphous minerals are present in significant concentrations. The widespread occurrence of iron, albeit at low levels, suggests it may be underrepresented in the mineralogical results. In these analyses, only heavily indurated samples have SiO_2 concentrations less than 80% with Al, P, Na, Ca, K, and S making up most of the balance.

4.2.2.4 Elemental Analyser results

The carbon and sulphur content of 13 nests was analysed (Table 4) to determine the typical concentrations prior to pretreatment and to complement XRD and XRF results. The average carbon concentration across all 13 samples is 0.65% but this is inflated by the high oxalate concentration in the heavily indurated sample, D019. The average carbon concentration, excluding D019, is 0.22% and is a more representative estimate of the carbon in old nests. This is significantly less than the

average 1.2% carbon measured in modern wasp nests and probably reflects the loss of carbon as CO_2 gas from decayed organic matter in the early stages of nest diagenesis (Trumbore 2009: 49).

The sulphur concentrations are broadly consistent with the XRD results. The five samples with the lowest sulphur concentrations (from 0.11% to 0.51%) also recorded no sulphate minerals in the XRD analysis. The eight higher sulphur concentration (0.63 – 2.87%) samples all recorded at least trace levels of sulphates in the XRD results.

Sample	**C%**	**S%**	Corrected $\delta^{13}C_{PDB}$
D019	5.75	1.80	-11.4
D105	0.07	2.04	-18.0
D119	0.70	0.11	-20.8
D131	0.11	2.59	-10.6
D134	0.12	2.87	-17.4
D136	0.10	1.87	-12.5
D144	0.15	0.63	-9.9
D147	0.25	1.50	-13.1
D152	0.25	0.35	-13.9
D161A	0.34	0.91	-20.7
D161B	0.21	0.24	-20.6
D168	0.25	0.46	-19.4
D348	0.10	0.51	-14.2
Mean:	0.65	1.22	-15.6

Table 4 Percentage weight of carbon and sulphur in old wasp nests and isotopic compositions of carbon.

4.2.3 Pretreatment

4.2.3.1 Carbon mass

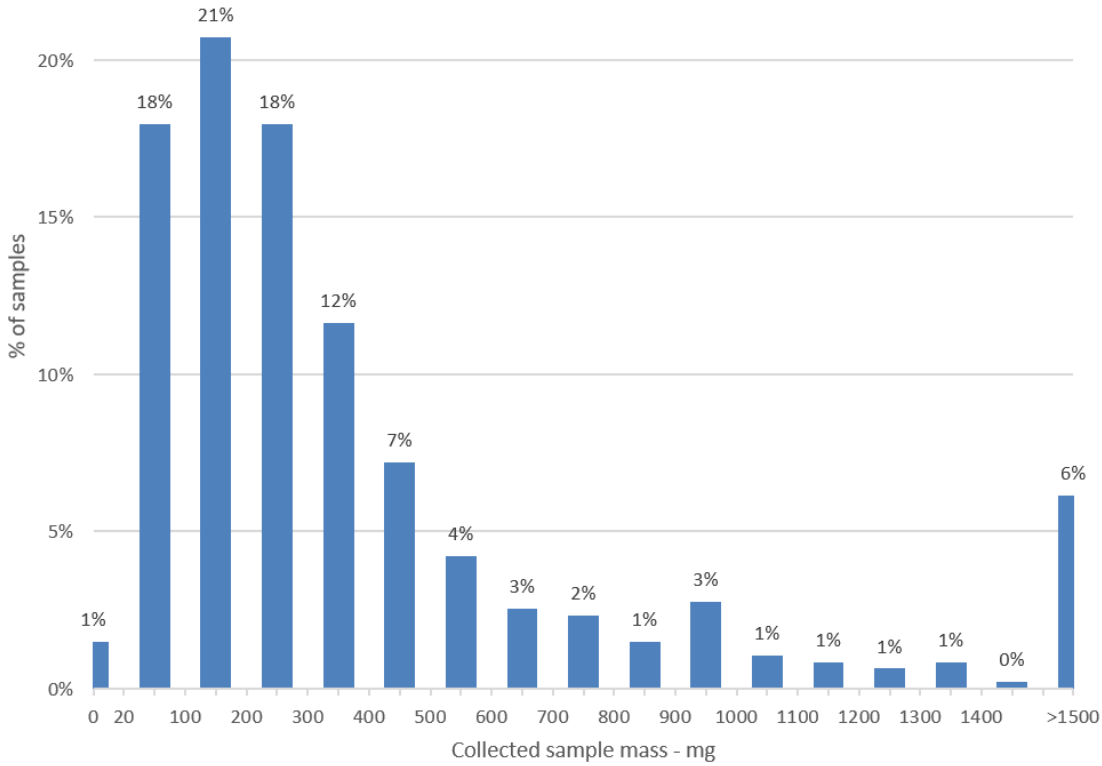

Figure 7 Histogram of the mass, as collected, of all old wasp nests included in this study

The median mass of all old wasp nests collected is 247 mg with 80% of samples having a mass of less than 570 mg (Figure 7). Of all the old wasp nests collected, 120 have been prepared for radiocarbon dating so far. A total of 175 sample fractions were prepared from these 120 samples. Initially, samples were pretreated using a standard ABA protocol (Standard ABA series in Figure 8). About 40% of these fractions yielded less than 12µg C after combustion (or failed during graphitisation) and were not measured. Experiments using HLS were then undertaken with the initial aim of improving the percentage of samples that produced sufficient carbon for dating.

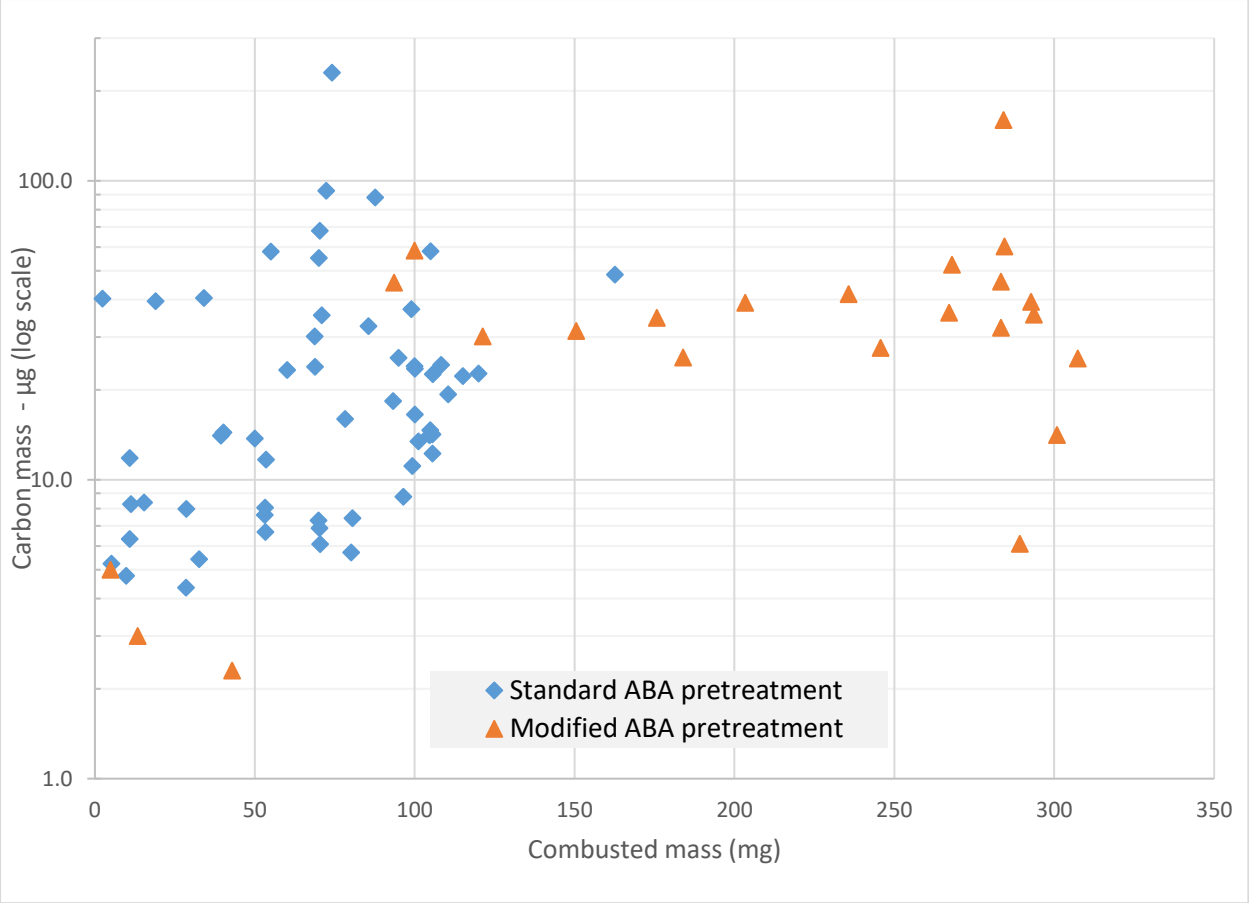

Figure 8 Mass of sample combusted vs carbon mass after sample combustion.

4.2.3.2 Heavy liquid separation

To improve the yield, experiments were conducted using HLS, on the assumption that charcoal would be concentrated in the light fraction providing the specific gravity was less than that of quartz (c. 2.6 g/cm^3). In practice, microscopic inspection of the heavy fractions suggested that they also contained a significant amount of microscopic charcoal. This was confirmed when both light and heavy fractions from 23 samples were combusted. The average amount of carbon in the heavy fractions (28µg) was very similar to that in the light fractions (31µg). Separations starting at a specific gravity of 1.2 and increasing up to 2.5 g/cm^3 established that the quantity of floating material (mostly charcoal) increased with density, suggesting pyrogenic carbon at varying degrees of mineralisation was present. This result in mud wasp nests mirrors that found to occur in soils where pyrogenic carbon becomes attached to and impregnated with soil minerals over time (e.g. Bird et al. 2008, Bird et al. 2015, Brodowski et al. 2005). While HLS was only partly successful in concentrating charcoal into the

light fraction, dating the separate fractions provided important insights into the carbon sources within the samples.

Sample Code*	Laboratory Code	Pretreatment Sequence	Fraction	C mass µg	^{14}C years BP	Error (1σ)	Reliability Score	Single Nest?
DR006_05-1	OZT801U2	ABA - HLS	Light	18	Modern		2	Y
DR006_05-1	OZT801U1	ABA - HLS	Heavy	13	3,110	140	1	Y
DR013_09-1	OZT797U*	ABA	All	48	11,530	80	5	N
DR013_09-1	OZT797U2	ABA - HLS	Light	110	16,930	100	7	N
DR013_09-1	OZT797U1	ABA - HLS	Heavy	26	15,940	160	3	N
DR013_11-1	OZT798U2	ABA - HLS	Light	51	4,920	80	7	N
DR013_11-1	OZT798U1	ABA - HLS	Heavy	20	11,350	150	3	N
DR015_06-1	OZT799U*	ABA	All	24	2,260	100	3	N
DR015_06-1	OZT799U1	ABA - HLS	Heavy	12	9,460	170	1	N

Table 5 Old wasp nests with multiple analysed fractions using initial pretreatment process. The sample code is constructed from a short site identifier, followed by a number to identify the painted motif and then the number of the sample collected (on that motif, at that site) in the format "SITE_MOTIF-NEST". Sample OZT797U2 has a measured δ13C of -22.5‰, all other samples are assumed to be -25‰.

Initially, 4 heavy/light fraction pairs were dated after the standard ABA pretreatment followed by HLS (Table 5). The results show some large differences between ages of the heavy and light fractions of the same sample, with the heavy fraction usually older. Only very large samples produced enough carbon for these experiments. Such samples often comprise nests of very different ages so extreme differences in the ages of the heavy and light fractions are feasible. Even so, some of the samples were clearly from a single generation nest ("Single Nest?" = Y in Table 6) so this is not the only cause. It may also be the case that the carbon masses were too low to produce reliable age estimates, so experiments were conducted on further samples using different pretreatment protocols (Table 6).

Sample Code	Laboratory Code	Pretreatment Sequence	Fraction	C mass µg	^{14}C years BP	Error (1σ)	Reliability Score	Single Nest?
DR013_06-1	OZT447	ABA	All	15	15,350	200	3	N
DR013_06-1	OZU776U1	A-HLS-BA(8M)	Light	27	10,820	120	7	N
DR013_06-1	OZU776U2	A-HLS-BA(8M)	Heavy	33	11,340	90	7	N
DR013_11-1	OZU777U1	A-HLS-BA(8M)	Light	43	1,370	610	8	N
DR013_11-1	OZU777U2	A-HLS-BA(8M)	Heavy	40	11,170	80	8	N
DR013_11-1	OZW354	A-HF-HLS-BA(8M)	Light	11	15,780	200	5	N
DR013_11-1	OZW355	A-HF-HLS-BA(8M)	Heavy	13	10,190	110	5	N
DR015_04-2	OZU778U1	A-HLS-BA(8M)	Light	17	7,010	90	5	N
DR015_04-2	OZU778U2	A-HLS-BA(8M)	Heavy	51	10,010	80	8	N
DR015_10-2	OZU779U1	A-HLS-BA(8M)	Light	42	14,200	110	9	N
DR015_10-2	OZU779U2	A-HLS-BA(8M)	Heavy	47	14,390	100	8	N
DR015_10-7	OZW379	A-HLS-BA(8M)	Light	11	4,690	90	2	N
DR015_10-7	OZW380	A-HLS-BA(8M)	Heavy	33	10,730	70	4	N
DR015_14-4	OZU780U1	A-HLS-BA(8M)	Light	11	12,420	150	5	N
DR015_14-4	OZU780U2	A-HLS-BA(8M)	Heavy	49	13,450	90	8	N
DT1207_01-1	OZW382	A-HLS-BA(8M)	Light	17	2,380	80	5	Y
DT1207_01-1	OZW383	A-HLS-BA(8M)	Heavy	21	6,870	70	6	Y
DT1207_12-1	OZW388	A-HLS-BA(8M)	Light	15	5,260	80	5	Y
DT1207_12-1	OZW389	A-HLS-BA(8M)	Heavy	22	8,240	80	6	Y
FW014_01-1	OZT444	ABA	All	93	5,820	70	8	Y
FW014_01-1	OZT455	ABA	All	87	5,150	70	7	Y
FW014_01-1	OZW352	A-HF-HLS-BA(8M)	Light	61	1,895	40	7	Y
FW014_01-1	OZW353	A-HF-HLS-BA(8M)	Heavy	13	2,560	70	3	Y
KG002_02-1	OZU781U1	A-HLS-BA(8M)	Light	120	13,030	80	9	N
KG002_02-1	OZU781U2	A-HLS-BA(8M)	Heavy	44	10,010	60	7	N
KG021A_02-2	OZU782U1	A-HLS-BA(8M)	Light	56	16,940	120	9	N
KG021A_02-2	OZU782U2	A-HLS-BA(8M)	Heavy	47	12,970	80	7	N
KG028A_03-1	OZU785U1	A-HLS-BA(8M)	Light	25	12,590	200	6	N
KG028A_03-1	OZU785U2	A-HLS-BA(8M)	Heavy	41	11,750	80	7	N

Table 6 Old wasp nests with multiple dated fractions using a range of modified pretreatment processes (except OZT447, OZT444, OZT455; included for comparison only).

The first experiment used a concentrated (8M or 16M HCl) final acid treatment in place of 2M HCl. Hedges et al (1998: 36) found that “routine acid treatment” did not remove all oxalate from two

pigment samples and Armitage et al (2001: 474) concluded that an anomalous result on a pigment date was due to incomplete removal of oxalates and/or carbonates. To test whether the 8/16M final acid step in the ABA process was removing acid soluble carbon, about 20% of the HCl supernatant was removed and dried down in small combustion tubes. The small tube was then combusted inside a larger sealed silica tube. The amount of carbon in 14 of these “acid soluble fractions” was measured to be in the range of 2.4 to 7.8µg with a mean of 5.3µg. This fraction may include up to 6µg of exogenous carbon as the inner/outer tube combustion method is known to be more susceptible to contamination, but 5 samples contained more than 7µg of carbon suggesting it cannot all be from contamination. The implication is that at least a third of samples contained 5 to 10 µg of acid soluble carbon in the final acid supernatant that was not removed in the first acid treatment. To ensure complete removal of oxalates, all subsequent samples (with Lab Codes following OZU272) used 8 or 16 M HCL in the final acid step.

Other changes to the pretreatment process included the use of larger combustion tubes when more than 100 mg of pretreated sample was available. The larger tubes were loaded with up to 300 mg of sample so many more contained enough carbon for AMS measurement (Figure 8).

4.2.4 Quality Control

In addition to chemical procedural blanks routinely used at ANSTO, five “modern” and “ancient” pseudo-nest samples were analysed to check for potential contamination introduced during pretreatment (Table 7). The 3 modern pseudo-nest analyses recorded pMC values within one standard deviation of the modern charcoal (OZV994) used to make this pseudo-nest material. This confirms that no significant undetected old carbon contamination occurred in the pretreatment process. Of the two old pseudo-nest analyses, one had no significant modern carbon contamination but the other had enough contamination to reduce the measured age to 42.7 – 41.7 cal ka BP. No specific source was identified for this abnormal result but given that routine blanks and standards showed no such contamination it is most likely that it occurred due to human error during ABA processing. More frequent use of an ancient pseudo-nest reference sample is recommended as an additional check for potential contamination during the earlier stages of sample processing.

Laboratory Code	Sample Description	Pretreatment Sequence	Fraction	C mass µg	$\delta^{13}C$ ‰	Error (1σ) ±	percent Modern Carbon	Error (1σ) ±	^{14}C years BP	Error (1σ) ±
OZV994	Modern charcoal only	ABA	All	-	-28.5	0.1	103.45	0.27	Modern	
OZW340	Modern pseudo-nest	A-HLS-BA(8M)	Light	31			103.46	0.59	Modern	
OZW342	Modern pseudo-nest	A-HLS-BA(8M)	Light	63			102.72	0.49	Modern	
OZW363	Modern pseudo-nest	A-HF-BA(16M)	All	52			103.44	0.44	Modern	
OZW362	Dead pseudo-nest	A-HF-BA(16M)	All	265	-24.5	0.4	0.07	0.04	>52600	
OZW424U2	Dead pseudo-nest	ABA(16M)	All	210			0.89	0.04	37,940	350

Table 7 Dated modern and ancient carbon pseudo-nest samples

4.2.5 Reliability Assessment

The preceding results and analysis identified three factors that affect the reliability of the ages measured: (i) mass of carbon analysed, (ii) ability to remove surface contamination and (iii) use of strong acid to remove all oxalates and carbonates. The nature of these factors means they cannot readily be quantified and included in a statistical error calculation. Nonetheless, an age estimate is more, or less likely to approximate the construction date of the nest depending on these factors (and potentially others). To record and summarise these differences a “Reliability Score” was devised and has been calculated for each AMS measurement reported herein. In this context, a more reliable age estimate is one that is closer to the true date of construction of the mud wasp nest.

The Reliability Score is the sum of semi-quantitative sub-scores for each of the three factors: carbon mass, physical pretreatment and chemical pretreatment. The score is an open-ended scale but, with current processes, the most reliable measurement scores a 10 (5+3+2, as follows). Half of the score weighting is for the mass of carbon analysed. Samples with < 12 µg C score zero, 1 for those between 12 and <20 µg, 2 for 20 to <30 µg and so on up to a score of 5 for samples of 50 µg or more. Optimal physical pretreatment scores a maximum of 3 for samples where the entire external surface can be ground off. At the other extreme, sand like samples that cannot be ground, scraped or ultrasonicated score a zero. The maximum score for chemical pretreatment is 2 when the protocol involving the use of 8/16M HCl is employed to generate a light fraction, and a score of zero applies to heavy fractions where oxalates may not have been completely removed.

The Reliability Scores listed in Tables 6 and 7 serve to identify results that may have an “anomalous sample composition” (sensu Taylor and Southon 2012: 979). As a relative scale, it is intended as an

aid to subsequent analysis of the relationship between the date as measured and the underlying or overlying rock art. For example, experiments on the multi-generation nest sample DR013_06-1, from underneath pigment, yielded 3 age estimates (top 3 rows of Table 6) so the question arises as to which date to use as a maximum age for the overlying pigment. An earlier date of 15,350 yr BP on part of the sample has a score of 3 and is discounted as less reliable in favour of a date of 10,820 yr BP on a light fraction with a score of 7. The heavy fraction, measured at 11,340 yr BP, also has a score of 7 so there is certainly charcoal of different ages in this sample, but it is the youngest charcoal that defines the maximum age for the overlying pigment. Hence the 10,820 yr BP date is selected as the most relevant maximum age for this sample.

4.2.6 Wasp nest age determinations

Of the 120 old nests processed to date, a total of 75 old wasp nest samples were successfully radiocarbon dated; 45 nests contained too little carbon for AMS measurement. Where multiple fractions from the same nest have been measured, one has been selected as the most appropriate as outlined in section 4.2.5. Measured wasp nest ages range from Modern to just over 20 cal ka BP. The results will be presented in detail elsewhere in the context of their relationship to rock art, but they are summarised graphically in Figure 9 simply to illustrate the range and estimated precision of ages obtained using the methods detailed here.

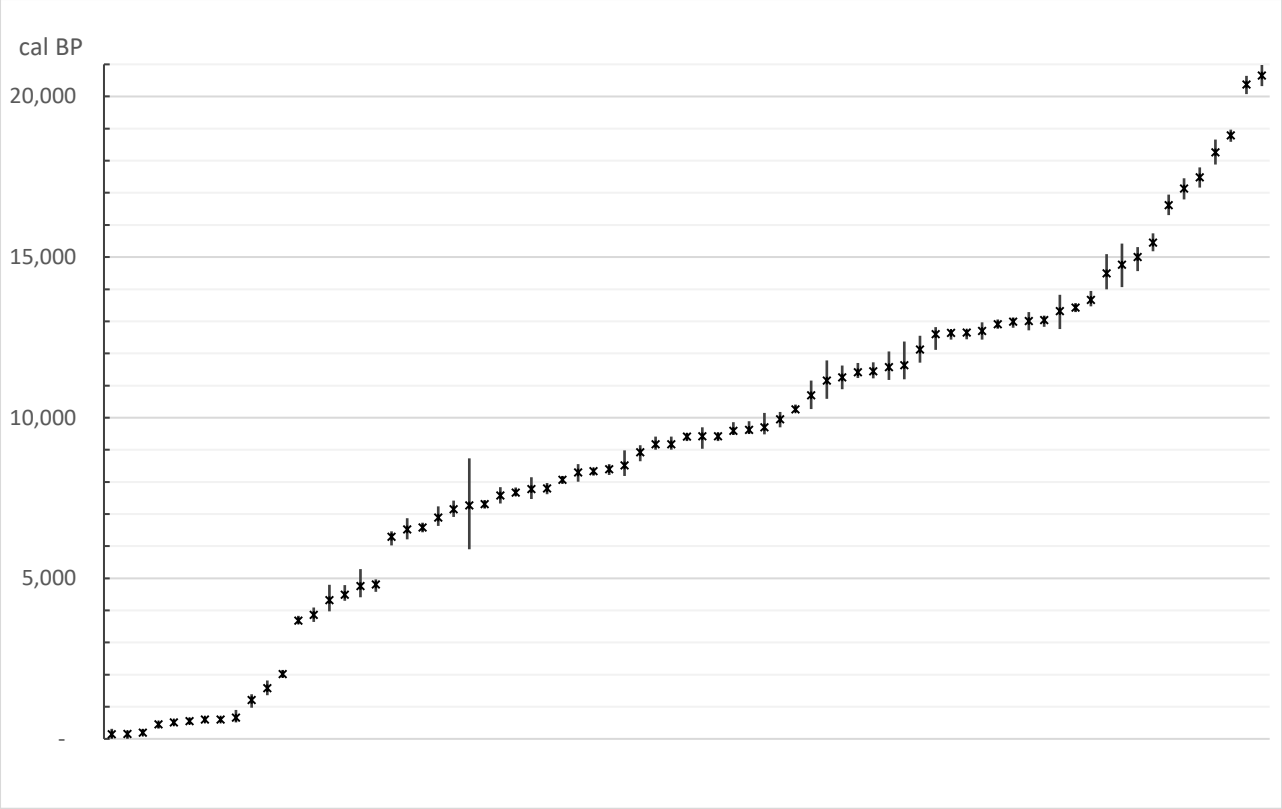

Figure 9 Median calibrated age (x) of wasp nest samples and 95.4% probability range (bar) (OxCal v4.3.2 SHCal13)

5 Discussion

The variations observed in the age of carbon in modern nests and the dates of different fractions prepared from old nests raise some key issues that are discussed in more detail below.

5.1 Charcoal as a target for dating nests

Analysis of the composition of the modern wasp nests suggested that charcoal was the main source of carbon likely to survive for long periods. Charcoal will generally be present in sediment collected by mud wasps. Currently, an average of 30% of the North Kimberley is burnt each year in bushfires (Vigilante et al. 2004) so pyrogenic carbon is abundant in this environment. The palaeoenvironmental record also suggests significant levels of burning, at least since people first arrived (Kershaw 1986: 48, Proske et al. 2014: 172). While plant material is another major carbon-bearing component in mud collected by wasps, it rapidly oxidizes to CO_2 and less stable organic compounds (Trumbore 2009:

49), some of which have a mean residence time in soils of just weeks to months (Kuzyakov 2006: 428).

Carbon isotope measurements on 5 modern nests (Table 1) point to short-lived grasses as a significant source of the organic content. The mean $\delta^{13}C$ value of -15.6‰ is significantly greater than the -26‰ expected for C_3 trees and shrubs. This suggests pyrogenic carbon from the locally abundant C_4 grasses (probably spinifex at -12‰ $\delta^{13}C$) or sedges (e.g. a regional Cyperaceae measured at -9.6‰ $\delta^{13}C$) are a major component of carbon in many nests (Hattersley 1983, Mcwilliam and Mison 1974, Wooller et al. 2005) in the Kimberley region. Ford et al. (1994: 62) studied the micromorphology of charcoal found in pigments from rock shelter walls in the Kimberley and also concluded the source was spinifex rather than wood.

Charcoal from these short-lived grasses will have a negligible inbuilt age prior to combustion and will usually be microscopic in scale, given the fine structure of grasses. It is also unlikely that wood in this region would have a significant inbuilt age, prior to combustion. The vegetation in the northern Kimberley Plateau is mostly savanna with eucalyptus woodlands, tall grasses and spinifex (Bowman et al. 2010: 205, Pepper and Scott Keogh 2014: 1447), and the trees are usually less than 200 years old (Ogden 1981: 418). It is possible, however, that older wood or charcoal is more common in rock shelters due to anthropogenic activity, but the action of ubiquitous termites and fire greatly limit the abundance of old wood.

The source of the old carbon detected in the modern nest samples, is therefore, most likely to be old charcoal present in surface sediments. This is consistent with findings from studies of soil organic carbon where the average age of pyrogenic carbon is reported to be of the order of centuries or a few millennia, with charcoals in tropical soils at the shorter end of that scale (Graetz and Skjemstad 2003: 41, Hobley et al. 2014a, 2014b: 751 and references therein).

With old carbon commonly present in the mud collected by wasps, how then can the radiocarbon age of incorporated charcoal be used to estimate the time of construction of the nest? One approach (Bronk Ramsey 2009b, Dee and Bronk Ramsey 2014: 83) notes that the age distribution of sampled charcoal is likely to be exponential (with most samples being young and the probability of selecting older samples diminishing as age increases). With a mean of 255 years (standard deviation of 370) from the 9 modern nest charcoal fractions dated (**Error! Reference source not found.**), an

exponential age distribution would imply that 95% of samples have an inbuilt age of less than 764 years (from the cumulative distribution function $P(X \leq x) = 1-\exp(-\lambda x)= 0.95$ where λ is 1/255). Dates on further charcoal fractions would improve this estimate of the inbuilt age of charcoal in newly constructed nests, but a reasonable working hypothesis is that the age of carbon in modern nests is most likely to be less than 764 years, and usually much less.

5.2 Alternative Methods

Alternative pretreatment methods were considered but the very small mass of carbon available in wasp nest samples means that most are not feasible. Old wasp nests measured had a carbon concentration of c. 0.2% and a median mass of 247 mg so a typical initial carbon mass is 0.5 mg. This is well below the more than 100 mg of well-preserved charcoal considered necessary for acid-base-oxidation-stepped combustion (ABOx-SC) processing (Higham et al. 2009a: 1265). The hydrogen pyrolysis (hypy) technique (Ascough et al. 2009, Ascough et al. 2010) also requires larger carbon masses and is not necessarily any more effective when the ages being measured are less than c. 25 ka (Higham et al. 2009b). The aim of pretreatment is to eliminate carbon-bearing minerals as well as organic contamination so techniques such as plasma oxidation offer no clear advantage over ABA in this application (Bird et al. 2010).

After standard ABA processing, the median carbon concentration is 0.022% (mean 0.077%) and for the modified ABA process, when HLS and 8/16M HCl is used, it is 0.019% (mean 0.022%). With some 90% of carbon being lost in chemical pretreatment, 10 nests were analysed to determine whether pollen, insect sclerites or other macroscopic carbon sources were viable targets, at least in very large samples. Even though these components are known to be in low abundance when the nest is constructed it may be that they are more able to survive pretreatment. Hydrofluoric acid was used to remove quartz from the largest samples (up to 7.7 g) after which the residue was microscopically inspected. None of these samples contained macroscopic particles and for those where pollen grains were evident their volume was minor compared to the volume of charcoal.

5.3 Sources of uncertainty

The sandstone-dominated geology of the northern Kimberley region is entirely devoid of limestone or soil carbonates, so potential contamination risks are more likely to be from modern rather than ancient carbon. Bednarik (2014: 230) also noted that there is little chance of old carbon contamination in the

absence of carbonates in the environment. It is possible that old, relatively insoluble, oxalate minerals may weather and mobilise across rock shelter surfaces by a process such as colloidal transport, but wasp nests are generally not built, or do not survive, on surfaces subject to run off. In the unlikely event that old oxalate minerals were mobilised onto wasp nests then they would be removed by strong acids during pretreatment. An important result of this study is thus that the identified contamination risks are such that true nest ages may be older than reported ages, but it is most unlikely that they are younger.

In the laboratory, the risk is also from modern carbon contamination as there are few sources of dead carbon contamination available, and these are generally known and controlled (e.g. grease from vacuum pumps). If the potential, uncontrolled, risks are predominantly from more modern carbon sources then the age estimates provided by wasp nests overlying rock art remain valid minimum ages: a contaminated sample may appear to be younger than the true age, but it will still be correct to state that the art must be older than the measured age of the nest.

The same is not true of under art nests: contamination from modern carbon could lead to an erroneous conclusion as the nest may now be measured to be younger than the art. This imposes an additional constraint on under art samples as they need to be such that any external surfaces can be thoroughly removed prior to ABA processing.

5.4 Anomalous results

Even with the revised pretreatment protocol (section 4.2.3.2) there are significant age differences between the heavy and light fractions in 15 of the 16 heavy/light sample pairs analysed (Table 6). For all but 4 samples, density separation had the effect of sorting the older, more mineralised pyrogenic carbon into the heavy fraction while the younger, less mineralised charcoal floated into the light fraction. Some of the samples, however, were single nests where all carbon should be of much the same age and yet the age differences were still significant. The greatest age differences occurred when it had not been possible to completely remove the outer surfaces prior to chemical processing, either because the sample pieces were too small or too friable. Samples where the outer surface was able to be thoroughly removed, such as DR015_10-2, DR015_14-4 and DR013_06-1, produced fractions with the smallest age differences. This outcome suggests carbon in detrital material and

accretions that form on the outer nest surfaces is not completely removed during chemical pretreatment alone, even with the most aggressive processes using strong acids.

The most likely source of this highly recalcitrant carbon is fine charcoal blown into rock shelters after the frequent bushfires. Consequently, carbon in light fractions should always be younger than that in heavy fractions and this is usually the case, but for four samples the opposite was true. Three of the four samples (KG002_02-1, KG021A_02-2, KG028A_03-1) are from the same river gorge area and are from sites that may, rarely, be flooded. It is possible that intermittent flooding acted to thoroughly bind younger detrital material to the mineral matrix so that it tended to sink during HLS, moving more of the younger carbon into the heavy fraction. All 4 samples were underneath pigment and the 3 with large age differentials between fractions were indurated nests well bonded to the underlying surface accretionary coating. Hence the sample included the older surface coating material as well as the original nest and subsequent accretionary deposits, all of which contain carbon of different ages. The age differential between fractions is plausible, even if the reason why the four light fractions are older is not certain.

5.5 Age distribution of dated nest samples

The spread of ages from 75 radiocarbon dates of old wasp nests across 20,000 years implies that wasp nests were produced with some regularity throughout this period (Figure 9). While it is possible that changes to environmental conditions affected the rate of nest production and preservation, most significant age ranges are represented in the data. From these initial results, there appears to be no major bias (apart from the normal taphonomic one) in the age distribution of nests that would lead to under-representation of periods of art production. A possible exception is the period 2 – 6 cal ka BP but that probably reflects some sampling bias toward older art styles and older nests. Given sufficient samples, dates on wasp nests should serve to constrain the age of all major art styles evident in this region over, at least, the last 20,000 years.

A reassuring result is the wide spread of ages of wasp nests from a single rock shelter site. If nest production was continuous rather than episodic (at a millennial scale) then there is a better chance that the age of any particular nest is close to the age of the underlying or overlying rock art. The single site with the largest number of dated nests is DR015 with 18 samples dated (Figure 10). Samples were not selected at random: if, based on colour, morphology, texture, and context, the nest appeared

to be young then it was unlikely to be sampled. If multiple samples are taken from such a site then a single, very old, date may be considered anomalous whereas multiple old dates from multiple samples increases confidence that the results are accurate. The 4 oldest nests have ages in the range 17 – 21 cal ka BP. Another 7 nests have ages in the range of 10 – 15 cal ka BP so more than half the nests dated are older than 10 ka. The overall range of dates leaves little doubt that nests were being built at this site in each millennium from 6 to 21 ka with a possible gap around 16±1 ka.

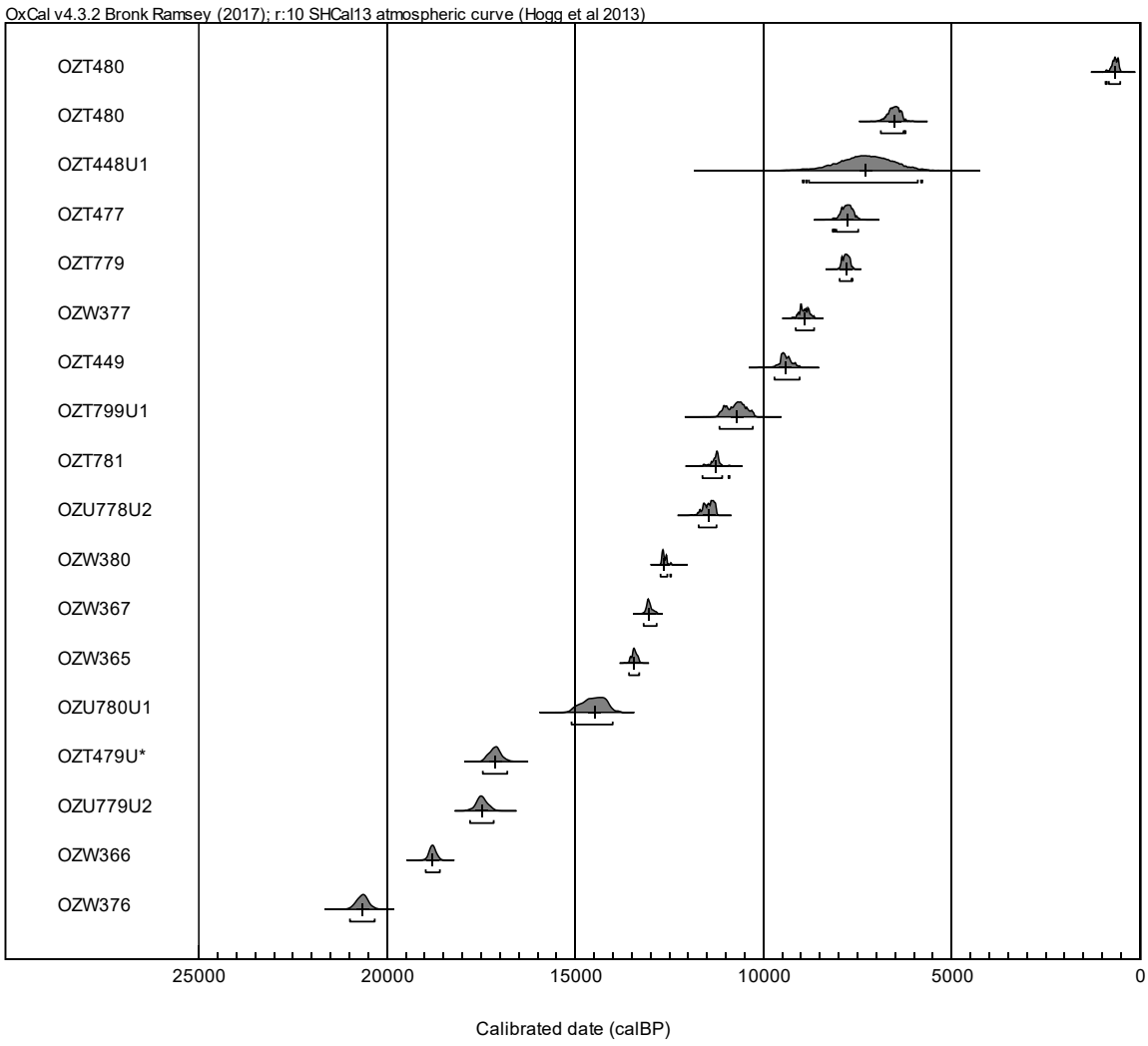

Figure 10 Calibrated ages for nests from site DR015 (95.4% probability range and median value)

6 Conclusion

The aim of this research has been to develop a robust approach to the radiocarbon dating of mud wasp nests to provide reliable bounding age estimates for rock art and other anthropogenic features on the surfaces of rock shelters.

The results establish that useful age estimates can be obtained when the following constraints are acknowledged:

- Charcoal is the carbon-bearing constituent most likely to provide a reliable radiocarbon age determination for old nests. Although some of the mud used to construct nests may contain a significant amount of old charcoal at the time of construction, it is possible to characterise this inbuilt age to determine the impact on the accuracy of age estimates for old nests. The potential non-analytical sources of uncertainty identified here will mostly be small (<10%) compared to such ages.
- While old, mineralised nests are closed to contamination, accretions form on outer surfaces and can trap younger detrital material. The modified chemical pretreatment protocol will remove carbon-bearing minerals but younger carbon contamination from aeolian charcoal or biological processes may remain. Dates on nests overlying the feature to be dated therefore provide reliable minimum age estimates as residual carbon contamination will only be younger than the age of the nest. Any nests underlying the same feature will be somewhat less reliable unless all possible contamination on the outer surface is removed prior to chemical pretreatment.
- The physical and chemical pretreatment protocols adopted, as well as the mass of carbon used for AMS measurement, all have an impact on the reliability of the age estimate of the wasp nest sample. Although the impact is difficult to quantify, the reliability assessment reported here communicates the relative level of confidence that can be held in one age measurement compared to another.

The results from 101 radiocarbon age determinations, on 75 old mud wasp nests, represent an unprecedented survey of the age of wasp nests in rock shelters. Of all the old nests, 31 are older than 10 cal ka BP and 9 are older than 15 cal ka BP with the two oldest nests dated to just over 20 cal ka BP. The wide range of ages measured establishes that, at the millennial scale, wasp nests have been

built quasi-continuously in the Kimberley over at least the last 20,000 years and are therefore, capable of providing age estimates for archaeological features and rock art throughout that period.

7 Acknowledgements

This research was funded by an Australian Research Council Linkage Projects LP130100501 and LP170100155 and co-funded by the Kimberley Foundation Australia and Dunkeld Pastoral Co Pty Ltd. DFinch is supported by an Australian Postgraduate Award and an AINSE Post Graduate Research Award.

We acknowledge and thank the Traditional Owners for permission to work on their country and for their support during fieldwork, particularly Augustine, Scott and Adrian Unghango, Ambrose Chalarimeri, Ian and Uriah Waina, Gareth, Ethan and Lucas Karadada on Balanggarra land and Donny and Kenny Woolagoodja and Wayne Rastus on Dambimangari land. Invaluable fieldwork support was provided by Helen Green, Cecilia Myers, Pauline Heaney, Susan Bradley, Paul Hartley, Nick Sundblom, Robin Maher, staff at Theda and Doongan Stations, Traudl Tan and Peter Kendrick. Special thanks also to the archaeologists who recorded the field context of our samples including Peter Veth, Sven Ouzman and Sam Harper.

It was only possible to visit so many remote sites in a relatively short time because modern day explorers, including Joc Schmiechen, the late Grahame Walsh, and the Kimberley Visions and Dunkeld Pastoral Co Pty Ltd Survey teams, have spent decades relocating and recording Kimberley rock art sites. We also received generous support from analytical technology experts from the University of Melbourne; Jon Woodhead, Alan Greig, Liz Goodall (XRD), Jay Black, Abaz Alimanovic and Graham Hutchinson, as well as Bin Yang (MCF), Alan Williams, Fiona Bertuch and the Radiocarbon Chemistry team at ANSTO. XRD measurements were performed at the Materials Characterisation and Fabrication Platform at the University of Melbourne. We acknowledge the help of radiocarbon laboratory staff and financial support for the Centre for Accelerator Science at ANSTO, through the Australian National Collaborative Research Infrastructure Strategy (NCRIS). We also thank two anonymous reviewers, whose comments led to substantial improvements to the manuscript.

8 References

Armitage, R. A., J. E. Brady, A. Cobb, J. R. Southon and M. W. Rowe (2001). "Mass spectrometric radiocarbon dates from three rock paintings of known age." American Antiquity **66**(3): 471-480.

Ascough, P. L., M. I. Bird, F. Brock, T. F. G. Higham, W. Meredith, C. E. Snape and C. H. Vane (2009). "Hydropyrolysis as a new tool for radiocarbon pre-treatment and the quantification of black carbon." Quaternary Geochronology **4**(2): 140-147.

Ascough, P. L., M. I. Bird, S. M. Francis and T. Lebl (2011). "Alkali extraction of archaeological and geological charcoal: evidence for diagenetic degradation and formation of humic acids." Journal of Archaeological Science **38**(1): 69-78.

Ascough, P. L., M. I. Bird, W. Meredith, R. E. Wood, C. E. Snape, F. Brock, T. F. G. Higham, D. J. Large and D. C. Apperley (2010). "Hydropyrolysis: Implications for radiocarbon pretreatment and characterization of black carbon." Radiocarbon **52**(3): 1336-1350.

Aubert, M. (2012). "A review of rock art dating in the Kimberley, Western Australia." Journal of Archaeological Science **39**(3): 573-577.

Bednarik, R. G. (2002). "The Dating of Rock Art: a Critique." Journal of Archaeological Science **29**(11): 1213-1233.

Bednarik, R. G. (2014). "Mud-wasp Nests and Rock Art." Rock Art Research **31**(2): 225-231.

Bird, M. I., P. L. Ascough, I. M. Young, C. V. Wood and A. C. Scott (2008). "X-ray microtomographic imaging of charcoal." Journal of Archaeological Science **35**(10): 2698-2706.

Bird, M. I., P. D. J. Charville-Mort, P. L. Ascough, R. Wood, T. Higham and D. Apperley (2010). "Assessment of oxygen plasma ashing as a pre-treatment for radiocarbon dating." Quaternary Geochronology **5**(4): 435-442.

Bird, M. I., J. G. Wynn, G. Saiz, C. M. Wurster and A. McBeath (2015). The Pyrogenic Carbon Cycle. Annual Review of Earth and Planetary Sciences, Vol 43. R. Jeanloz and K. H. Freeman. Palo Alto, Annual Reviews. **43:** 273-298.

Bowman, D., G. K. Brown, M. F. Braby, J. R. Brown, L. G. Cook, M. D. Crisp, F. Ford, S. Haberle, J. Hughes, Y. Isagi, L. Joseph, J. McBride, G. Nelson and P. Y. Ladiges (2010). "Biogeography of the Australian monsoon tropics." Journal of Biogeography **37**(2): 201-216.

Brock, F., D. G. Froese and R. G. Roberts (2010). "Low temperature (LT) combustion of sediments does not necessarily provide accurate radiocarbon ages for site chronology." Quaternary Geochronology **5**(6): 625-630.

Brodowski, S., W. Amelung, L. Haumaier, C. Abetz and W. Zech (2005). "Morphological and chemical properties of black carbon in physical soil fractions as revealed by scanning electron microscopy and energy-dispersive X-ray spectroscopy." Geoderma **128**(1–2): 116-129.

Bronk Ramsey, C. (2009a). "Bayesian analysis of radiocarbon dates." Radiocarbon **51**(1): 337-360.

Bronk Ramsey, C. (2009b). "Dealing with outliers and offsets in radiocarbon dating." Radiocarbon **51**(3): 1023-1045.

Bronk Ramsey, C. (2017). "Methods for Summarizing Radiocarbon Datasets." Radiocarbon: 1-25.

Dee, M. W. and C. Bronk Ramsey (2014). "High-Precision Bayesian Modeling of Samples Susceptible to Inbuilt Age." Radiocarbon **56**(1): 83-94.

Devries, H. L. and G. W. Barendsen (1954). "Measurements of age by the carbon-14 technique." Nature **174**(4442): 1138-1141.

Fink, D., M. Hotchkis, Q. Hua, G. Jacobsen, A. M. Smith, U. Zoppi, D. Child, C. Mifsud, H. van der Gaast, A. Williams and M. Williams (2004). "The ANTARES AMS facility at ANSTO." Nuclear Instruments and Methods in Physics Research Section B: Beam Interactions with Materials and Atoms **223–224**(0): 109-115.

Ford, B., I. MacLeod and P. Haydock (1994). "Rock Art Pigments from Kimberley Region of Western Australia: Identification of the Minerals and Conversion Mechanisms." Studies in Conservation **39**(1): 57-69.

Graetz, R. D. and J. Skjemstad (2003). The charcoal sink of biomass burning on the Australian continent, CSIRO Atmospheric Research.

Green, H., A. Gleadow and D. Finch (2017a). "Characterisation of mineral deposition systems associated with rock art in the Kimberley region of northwest Australia." Data in Brief.

Green, H., A. Gleadow, D. Finch, J. Hergt and S. Ouzman (2017b). "Mineral deposition systems at rock art sites, Kimberley, Northern Australia - Field observations." Journal of Archaeological Science-Reports **14**: 340-352.

Hatté, C., J. Morvan, C. Noury and M. Paterne (2001). "Is Classical Acid-Alkali-Acid Treatment Responsible for Contamination? An Alternative Proposition." Radiocarbon **43**(2A): 177-182.

Hattersley, P. W. (1983). "The distribution of C3 and C4 grasses in Australia in relation to climate." Oecologia **57**(1): 113-128.

Hedges, R. E. M., C. Bronk Ramsey, G. J. Van Klinken, P. B. Pettitt, C. Nielsen-Marsh, A. Etchegoyen, J. O. F. Niello, M. T. Boschin and A. M. Llamazares (1998). "Methodological issues in the C-14 dating of rock paintings." Radiocarbon **40**(1): 35-44.

Higham, T., F. Brock, M. Peresani, A. Broglio, R. Wood and K. Douka (2009a). "Problems with radiocarbon dating the Middle to Upper Palaeolithic transition in Italy." Quaternary Science Reviews **28**(13-14): 1257-1267.

Higham, T. F. G., H. Barton, C. S. M. Turney, G. Barker, C. B. Ramsey and F. Brock (2009b). "Radiocarbon dating of charcoal from tropical sequences: results from the Niah Great Cave, Sarawak, and their broader implications." Journal of Quaternary Science **24**(2): 189-197.

Hobley, E., G. R. Willgoose, S. Frisia and G. Jacobsen (2014a). "Stability and storage of soil organic carbon in a heavy-textured Karst soil from south-eastern Australia." Soil Research **52**(5): 476-482.

Hobley, E., G. R. Willgoose, S. Frisia and G. Jacobsen (2014b). "Vertical distribution of charcoal in a sandy soil: evidence from DRIFT spectra and field emission scanning electron microscopy." European Journal of Soil Science **65**(5): 751-762.

Hogg, A. G., Q. Hua, P. G. Blackwell, M. Niu, C. E. Buck, T. P. Guilderson, T. J. Heaton, J. G. Palmer, P. J. Reimer, R. W. Reimer, C. S. M. Turney and S. R. H. Zimmerman (2013). "SHCal13 Southern Hemisphere calibration, 0–50,000 years cal BP." Radiocarbon **55**(4): 1889-1903.

Hua, Q., G. E. Jacobsen, U. Zoppi, E. M. Lawson, A. A. Williams, A. M. Smith and M. J. McGann (2001). "Progress in radiocarbon target preparation at the ANTARES AMS Centre." Radiocarbon **43**(2A): 275-282.

Hua, Q., U. Zoppi, A. A. Williams and A. M. Smith (2004). "Small-mass AMS radiocarbon analysis at ANTARES." Nuclear Instruments & Methods in Physics Research Section B-Beam Interactions with Materials and Atoms **223**: 284-292.

Kershaw, A. P. (1986). "Climatic change and Aboriginal burning in north-east Australia during the last two glacial/interglacial cycles." Nature **322**(6074): 47-49.

Klingner, S., F. Voigts, W. Viol and W. Maus-Friedrichs (2013). "Analysis of plasma degreased aluminium foil with XPS." Surface Engineering **29**(5): 396-401.

Kuzyakov, Y. (2006). "Sources of CO2 efflux from soil and review of partitioning methods." Soil Biology and Biochemistry **38**(3): 425-448.

Mcwilliam, J. and K. Mison (1974). "Significance of the C4 Pathway in *Triodia irritans* (Spinifex), a Grass Adapted to Arid Environments." Functional Plant Biology **1**(1): 171-175.

Morwood, M., G. Walsh and A. L. Watchman (1994). "The dating potential of rock art in the Kimberley, NW Australia." Rock Art Research: The Journal of the Australian Rock Art Research Association (AURA) **11**(2): 79.

Naumann, I. D. (1983). The biology of mud nesting Hymenoptera (and their associates) and Isoptera in rock shelters of the Kakadu region, Northern Territory. The Rock Art Sites of Kakadu National Park - Some Preliminary Research Findings for their Conservation and Management. D. Gillespie. Canberra, Australian National Parks and Wildlife Service**:** 127 - 189.

Ogden, J. (1981). "Dendrochronological Studies and the Determination of Tree Ages in the Australian Tropics." Journal of Biogeography **8**(5): 405-420.

Pepper, M. and J. Scott Keogh (2014). "Biogeography of the Kimberley, Western Australia: a review of landscape evolution and biotic response in an ancient refugium." Journal of Biogeography **41**(8): 1443-1455.

Polidori, C., L. Trombino, C. Fumagalli and F. Andrietti (2005). "The nest of the mud-dauber wasp, Sceliphron spirifex (Hymenoptera, Sphecidae): application of geological methods to structure and brood cell contents analysis." Italian Journal of Zoology **72**(2): 153-159.

Proske, U., D. Heslop and S. Haberle (2014). "A Holocene record of coastal landscape dynamics in the eastern Kimberley region, Australia." Journal of Quaternary Science **29**(2): 163-174.

Ridges, M., I. Davidson and D. Tucker (2000). The organic environment of paintings on rock. Advances in Dating Australian Rock-Markings: Papers from the First Australian Rock-Picture Dating Workshop, Lucas Heights, The Australian Rock Art Research Association.

Roberts, R., G. Walsh, A. Murray, J. Olley, R. Jones, M. Morwood, C. Tuniz, E. Lawson, M. Macphall, D. Bowdery and I. Naumann (1997). "Luminescence dating of rock art and past environments using mud-wasp nests in northern Australia." Nature **387**(6634): 696-699.

Roberts, R. G., G. L. Walsh, J. M. Olley, A. S. Murray, M. K. Macphail, I. D. Naumann, R. Jones and M. J. Morwood (2000). Rock-picture chronologies and palaeoenvironmental records from fossil mud-wasp nests: preliminary investigations using optical dating. Advances in Dating Australian Rock-Markings. First Australian Rock-Picture Dating Workshop. G. Ward and C. Tuniz. Lucas Heights, Australian Rock Art Research Association**:** 40-44.

Ross, J., K. Westaway, M. Travers, M. J. Morwood and J. Hayward (2016). "Into the Past: A Step Towards a Robust Kimberley Rock Art Chronology." PLoS ONE **11**(8): e0161726.

Taylor, R. E. and J. Southon (2012). "On the Resolution of 14C Dating Anomalies: Case Studies from New World Archaeology." Radiocarbon **54**(3-4): 979-991.

Trumbore, S. (2009). "Radiocarbon and Soil Carbon Dynamics." Annual Review of Earth and Planetary Sciences **37**(1): 47-66.

Vigilante, T., D. Bowman, R. Fisher, J. Russell-Smith and C. Yates (2004). "Contemporary landscape burning patterns in the far North Kimberley region of north-west Australia: human influences and environmental determinants." Journal of Biogeography **31**(8): 1317-1333.

Watchman, A. (2000). "A review of the history of dating rock varnishes." Earth-Science Reviews **49**: 261 - 277.

Wilcken, K., M. Hotchkis, V. Levchenko, D. Fink, T. Hauser and R. Kitchen (2015). "From carbon to actinides: A new universal 1MV accelerator mass spectrometer at ANSTO." Nuclear Instruments & Methods in Physics Research Section B-Beam Interactions with Materials and Atoms **361**: 133-138.

Wooller, M. J., B. J. Johnson, A. Wilkie and M. L. Fogel (2005). "Stable isotope characteristics across narrow savanna/woodland ecotones in Wolfe Creek Meteorite Crater, Western Australia." Oecologia **145**(1): 100-112.

Yang, B. and A. M. Smith (2016). "Conventionally Heated Microfurnace for the Graphitization of Microgram-Sized Carbon Samples." Radiocarbon **59**(3): 859-873.

Yang, B., A. M. Smith and Q. Hua (2013). "A cold finger cooling system for the efficient graphitisation of microgram-sized carbon samples." Nuclear Instruments & Methods in Physics Research Section B-Beam Interactions with Materials and Atoms **294**: 262-265.

Yoshida, H., R. G. Roberts and J. M. Olley (2003). "Progress towards single-grain optical dating of fossil mud-wasp nests and associated rock art in northern Australia." Quaternary Science Reviews **22**(10-13): 1273-1278.

This information is supplementary to the paper published in

Quaternary Geochronology:

New developments in the radiocarbon dating of mud wasp nests

Authors: Damien Finch, Andrew Gleadow, Janet Hergt, Vladimir A Levchenko, David Fink

DOI: https://doi.org/10.1016/j.quageo.2019.02.007

Supplementary Information

1. Experimental methods

1.1. **X-Ray Fluorescence** (XRF): 14 old wasp nest samples were prepared as fused glass disks using a mixed lithium metaborate/tetraborate flux and analysed on a SPECTRO Xepos energy dispersive XRF spectrometer in the School of Earth Sciences at the University of Melbourne. Calibrations were constructed using a wide variety of international certified reference materials (including United States Geological Survey (BCR-1, BCR-2, AGV-1, AGV-2, BIR-1, BHVO-1, BHVO-2, G-2, PCC-1), SARM (NIM-L, NIM-S, NIM-G, NIM-P), and the International Association of Geoanalysts (PM-S, WS-E)) and analyses of secondary reference materials suggest accuracy generally better than 1 - 2% for most elements. Analytical reproducibility is generally better than 1% for most elements with the exception of P_2O_5 (up to 2%) and Na_2O (up to 4%).

1.2. **X-ray diffraction** (XRD): 41 old wasp nest samples were measured using a Bruker D8 Advance x-ray powder diffractometer, part of the Materials Characterisation and Fabrication Platform at the University of Melbourne. The D8 uses Ni-filtered Cu kα radiation with an incident beam divergence of 0.26° and a 2.5° soller slit in the diffracted beam. Intensities were measured between angles of at least 5–85° 2θ, with a step size of 0.02° and a scan rate of 1.0 s per step. Mineral phases were identified and semi-quantified using Materials Data Inc. Jade 9.3 and Bruker EVA software linked to the ICDD PDF-2 and PDF- 4 databases with key phases established for each sample using standard search-matching procedures.

1.3. **Standard radiocarbon chemical pretreatment**: The first acid treatment used a 2M HCl solution added to the sample in the centrifuge tube then placed in a 60^{o}C shaking water bath for 2 hours after which it was rinsed in ultrapure water. The alkali treatment dissolves degraded organic material present in the form of humic acids (Ascough et al. 2011) as well as fats and proteins. NaOH, starting at 0.5% concentration, was added and the tube returned to the water bath for 1 hour. If the solution was clear, then the alkali treatment was repeated a final time. If the sample was not clear, the process was repeated at double the

concentration of NaOH, up to a maximum of 8%. After rinsing to a neutral pH. a 2M HCl acid solution was added then left to stand at room temperature for at least 2 hours. After rinsing, the sample was transferred into a glass vial and dried in an oven at 60°C.

1.4. **Graphitisation and AMS measurement**: The standard process and equipment used to convert most pretreated samples into graphite targets for accelerator mass spectrometry (AMS) measurement is described by Hua et al (2001) and (2004). Some 33 samples used essentially this process to convert carbon dioxide to graphite but employing ANSTO's microconventional furnace (MCF) facility, developed to more efficiently graphitise ultra-small samples (Yang and Smith 2016, Yang et al. 2013). The carbon isotope ratios of the graphite targets were then measured in one of three of ANSTO's Accelerator Mass Spectrometers (AMS); 10MV ANTARES, 2MV STAR or 1MV VEGA (Fink et al. 2004, Wilcken et al. 2015) against OxI and Ox II International Radiocarbon Standards.

Where surplus graphite remained after AMS measurement, the δ13C value was measured using an Elementar varioMICRO CUBE Elemental Analyser coupled to a Micromass Isoprime IRMS and age determinations were corrected accordingly (following Stuiver and Polach 1977). Where all graphite was consumed during AMS measurement the δ13C value was assumed to be -25.0‰, consistent with other measured samples.

2. Micro-CT scan of old wasp nest

An example of a three-dimensional density model generated by a micro-CT scan of an old wasp nest sample (D459) is included here as a video file (micro-CT scan D459.mp4). Each frame in the video represents a two-dimensional slice through the sample. Areas of highest density, such as pigment (rich in haematite), show up as white pixels and those of lowest density (air) as black pixels.

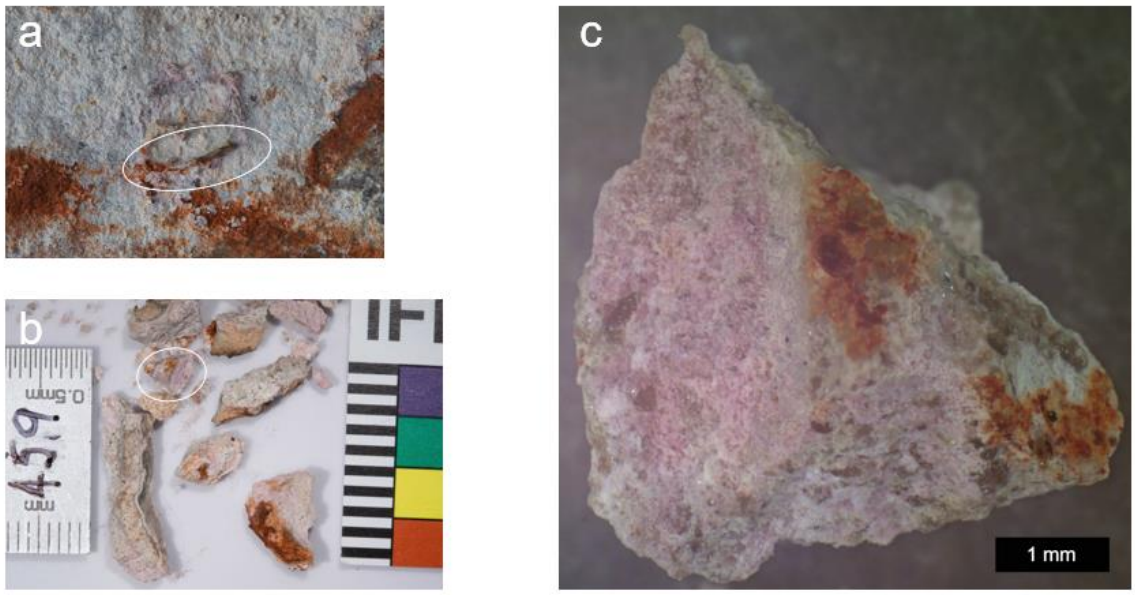

Figure 1 Mineralised wasp nest sample D459. (a) Pigment coated nest prior to sampling, (b) Sample as removed. Piece selected for scanning is circled, (c) plan view of scanned piece showing brown pigment coating.

3. Calibrated radiocarbon dates for modern wasp nest fractions

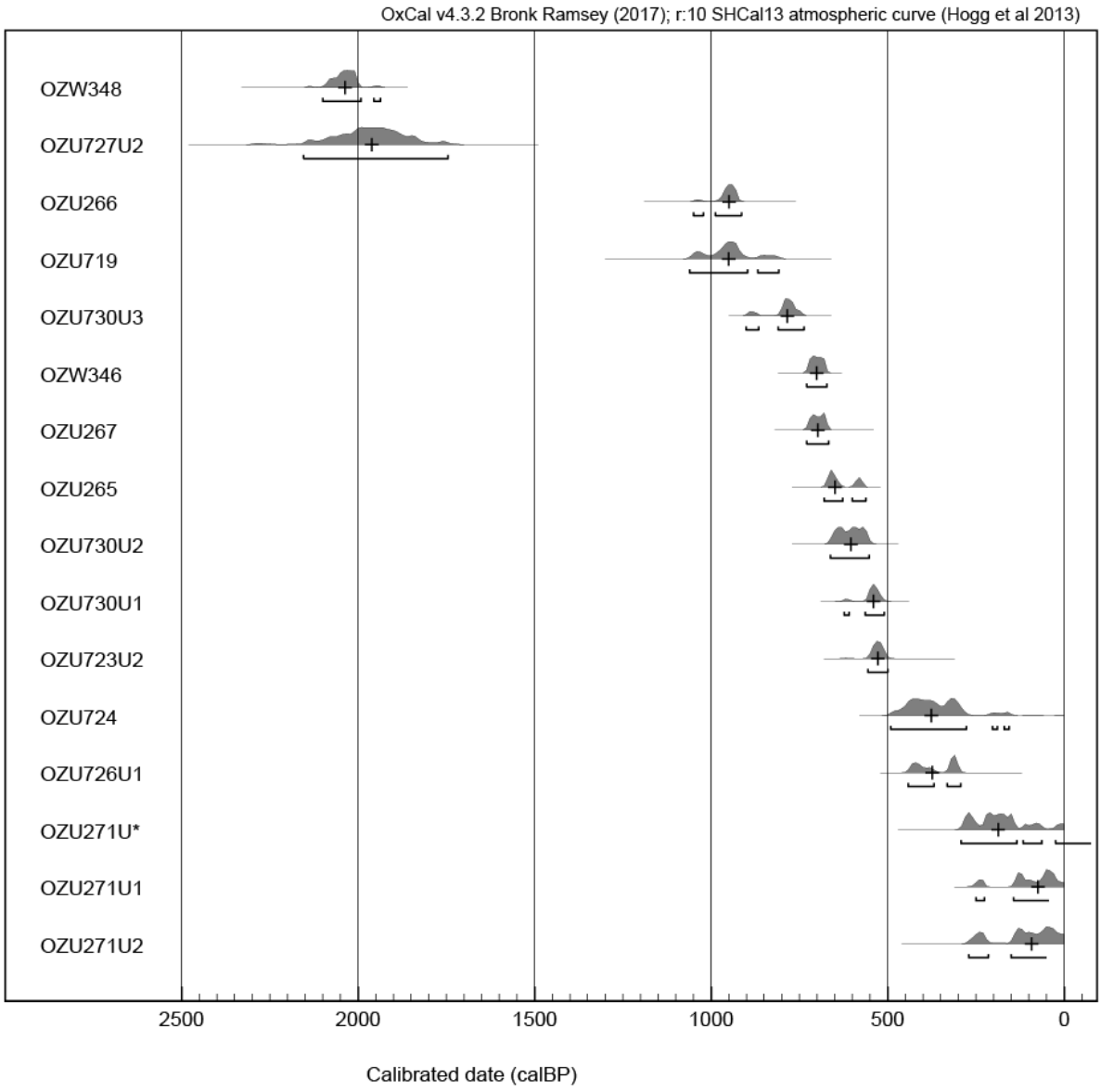

Figure 2 Calibrated radiocarbon date ranges (95.4%) and median for Modern Wasp Nests and associated mud sources.

4. Modern wasp nest AMS measurements

Sample Code	Laboratory Code	C mass µg	$\delta^{13}C$ ‰	Error (1σ)	percent Modern Carbon	Error (1σ)
D202	OZU719	97			87.33	0.54
D202	OZU720	3,070	-23.9	0.1	109.48	0.79
D204	OZU721	55			104.97	0.78
D204	OZU722	1,830	-23.7	0.4	112.98	0.33
D206	OZU723U1	170	-20.9		100.98	0.36
D206	OZU723U2	200			93.39	0.39
D207	OZU724	42			96.00	0.66
D208	OZU265	114	-23.2		91.23	0.33
D208	OZU266	570	-21.3	0.1	87.29	0.32
D208	OZU267	950	-22.9	0.1	90.37	0.26
D208	OZU268	170			105.59	0.33
D208	OZU730U1	470	-25.3	0.1	93.05	0.36
D208	OZU730U2	121	-22.6		91.89	0.46
D208	OZU730U3	430	-21.5	0.3	89.02	0.22
D209	OZU725	800	-24.5	0.1	107.98	0.37
D210	OZU269	2,000	-18.3	0.1	107.21	0.3
D211	OZU726U1	1,740	-23.8	0.1	96.13	0.27
D211	OZU726U2	520	-22.5	0.1	100.98	0.34
D212	OZU727U1	45			101.64	0.76
D212	OZU727U2	17			77.55	0.76
D213	OZU270	4,700	-23.6	0.1	109.33	0.34
D215	OZU271U*	850	-18.2	0.2	97.54	0.37
D215	OZU271U1	250	-17.3	0.2	98.60	0.3
D215	OZU271U2	45			98.79	0.59
D216	OZU728U1	410			103.81	0.36
D216	OZU728U2	170	-21.3		105.40	0.38
D217	OZU729U1	2,630	-26.1	0.1	134.66	0.47
D217	OZU729U2	270	-23.9	0.4	112.48	0.39
D219	OZU272	1,500	-23.1	0.1	102.69	0.3
D500	OZW346	1,900	-25.2	0.1	90.27	0.2
D508	OZW344	740	-25.1	0.2	107.62	0.25
D514	OZW347	250	-24.2		100.35	0.34
D632	OZW349	1,000	-25.9	0.1	104.35	0.24
D670	OZW350	71			104.77	0.5
D699	OZW345	46	-25.0		105.36	0.57
D516	OZW348	860	-24.9	0.1	76.91	0.23
D700	OZW351	1,780	-24.8	0.2	108.84	0.31

Table 1 Radiocarbon measurements for modern wasp nest and soil samples

Site:	FWC003	FWC010	FWC010	FWC016	FWC014	FWC014	FWC014	FWC019	DRY009	DRY008	DRY012C	DRY012C	DRY013	DRY013	DRY013	DRY013	DRY013	DRY013	DRY015	DRY015	DRY015	DRY015	DRY015	DRY015	DRY015	DRY015	DRY018	DRY016	DRY016	DRY016	DRY006	DRY006	DRY006	DRY006	DRY037	DRY041	KGR021A	PC15	PC15
XRD Sample:	D010	D018	D019	D020	D025	D026	D027a	D034	D105	D111	D118	D119	D129	D131	D134	D136	D139	D140o	D144	D147	D151	D152	D153	D154	D155	D335	D156A	D161A	D161B	D161C	D162	D164	D167B	D168	D348	D379	D459	PC15-01	PC15-02
Mineral	**Chemical Formula**																																						
Carbonates																																							
Calcite	$CaCO_3$							○								○																							
Nitrates																																							
Niter	KNO_3																																			○			
Nitratine	$NaNO_3$											○													○										●					
Oxalates																																							
Glushinskite	$C_2MgO_4{\cdot}2H_2O$				●																																		
Whewellite	$Ca(C_2O_4){\cdot}H_2O$		○	●	○					○																													
Oxides																																							
Hematite/Iron Oxide	Fe_2O_3											○												○						○							●			○
Phosphates, Arsenates																																							
Aluminum Ammonium Hydroxide Phosphate Hydrate	$Al_2(NH_4)(OH)(PO_4)_2(H_2O)_2$																										●	●		●									
Leucophosphite	KFe2(PO4)2(OH)(H2O)2												○									●																	
Taranakite	$K_3Al_5(HPO_4)_6(PO_4)_2{\cdot}18(H_2O)$							●				●			○							●		○										●			●		
Tinsleyite	$KAl_2(PO_4)_2(OH){\cdot}2(H_2O)$														●		○							●									○		●				
Silicates																																							
Illite	$K_{0.65}Al_{2.0}[Al_{0.65}Si_{3.35}O_{10}](OH)_2$													○												○													
Kaolinite	$Al_2(Si_2O_5)(OH)_4$	○				○		○										○							○														
Montmorillonite	$(Na,Ca)_{0.33}(Al,Mg)_2(Si_4O_{10})$					○																																	
Muscovite	$(K,Na)Al_2(Si,Al)_4O_{10}(OH)_2$											○			○		○														○		○						
Quartz	SiO_2	●	●	●	●	●	●	●	●	●	●	●	●	●	●	●	●	●	●	●	●	●	●	●	●	●	●	●	●	●	●	●	●	●	●	●	●	●	●
Sulphates																																							
Alunite	$KAl_3(SO_4)_2(OH)_6$									○									○	○										○	○					●			
Anhydrite	$CaSO_4$										○				○	○																							
Bassanite	$CaSO_4{\cdot}0.5H_2O$																							○															
Boussingaultite	$(NH_4)_2Mg(SO_4)_2{\cdot}6(H_2O)$												○																										
Gypsum	$CaSO_4{\cdot}2H_2O$		●	●	○		○		●		●																	○										
Polyhalite	$K_2Ca_2Mg(SO_4)_4{\cdot}2H_2O$												○	○		○									○											○	●		
Schlossmacherite	$(H_3O)_{0.75}Ca_{0.25}Al_3(AsO_4)_{1.5}(SO_4)_{0.5}(OH)_6$												○	○											○							○						○	

Key:

Major phase (100 - 16%)	●
Minor Phase (15 - 4%)	○
Trace (<4%)	○

Table 2 Mineral composition of old wasp nests - XRD results

5. References

Ascough, P. L., M. I. Bird, S. M. Francis and T. Lebl (2011). "Alkali extraction of archaeological and geological charcoal: evidence for diagenetic degradation and formation of humic acids." Journal of Archaeological Science **38**(1): 69-78.

Fink, D., M. Hotchkis, Q. Hua, G. Jacobsen, A. M. Smith, U. Zoppi, D. Child, C. Mifsud, H. van der Gaast, A. Williams and M. Williams (2004). "The ANTARES AMS facility at ANSTO." Nuclear Instruments and Methods in Physics Research Section B: Beam Interactions with Materials and Atoms **223–224**(0): 109-115.

Hua, Q., G. E. Jacobsen, U. Zoppi, E. M. Lawson, A. A. Williams, A. M. Smith and M. J. McGann (2001). "Progress in radiocarbon target preparation at the ANTARES AMS Centre." Radiocarbon **43**(2A): 275-282.

Hua, Q., U. Zoppi, A. A. Williams and A. M. Smith (2004). "Small-mass AMS radiocarbon analysis at ANTARES." Nuclear Instruments & Methods in Physics Research Section B-Beam Interactions with Materials and Atoms **223**: 284-292.

Stuiver, M. and H. A. Polach (1977). "Reporting of ^{14}C Data - Discussion." Radiocarbon **19**(3): 355-363.

Wilcken, K., M. Hotchkis, V. Levchenko, D. Fink, T. Hauser and R. Kitchen (2015). "From carbon to actinides: A new universal 1MV accelerator mass spectrometer at ANSTO." Nuclear Instruments & Methods in Physics Research Section B-Beam Interactions with Materials and Atoms **361**: 133-138.

Yang, B. and A. M. Smith (2016). "Conventionally Heated Microfurnace for the Graphitization of Microgram-Sized Carbon Samples." Radiocarbon **59**(3): 859-873.

Yang, B., A. M. Smith and Q. Hua (2013). "A cold finger cooling system for the efficient graphitisation of microgram-sized carbon samples." Nuclear Instruments & Methods in Physics Research Section B-Beam Interactions with Materials and Atoms **294**: 262-265.